ADVANCED ENERGY MATERIALS
www.advenergymat.de

Luminescent Solar Collectors: Quo Vadis?

Jean Roncali

Luminescent solar concentrators (LSCs) are optical systems that absorb, convert, and concentrate solar light by means of photoluminescence of an emitting material embedded in a transparent waveguide. LSCs combine large possibilities of variation of shape, flexibility, color, and transparency and can operate under direct or diffuse light. LSCs were actively investigated in the period 1975–1985 in view of photovoltaic (PV) conversion. After 20 years of sleep, research on LSCs has reemerged in the first years of the millennium driven by their potential application for PV conversion in built environment. Research on LSCs aims at the development of new active and passive components, namely emitting and light-guiding materials, and at the reduction of the loss factors associated with the elemental processed involved in the operation in order to improve power conversion efficiency. After a brief historical account, the operating principles, characterization, components, technology, and applications are reviewed. Finally, the performance of LSCs are critically discussed in a global perspective with particular emphasis on the basic contradiction between light concentration and conversion efficiency leading to some suggestions for future development of the topic.

1. Introduction

Solar energy is expected to play a major role in a context strongly marked by an increasing energy demand, the imperative reduction of carbon emissions, and increasing environmental concerns. The photovoltaic (PV) conversion of solar light is an area of intense research activity. Whereas the industry of solar modules based on silicon PV cells underwent an impressive development over the past half century, this development is accompanied by a parallel intensification of research on alternative technologies in view of reducing the cost and environmental impact of PV conversion. Besides, a continuous improvement of PV cells based on inorganic semiconductors, dye-sensitized solar cells (DSSCs), organic photovoltaic cells, and more recently perovskites cells are a focus of intense research effort. Based on a quasi-linear relationship between the power of the incident light and the intensity of the photogenerated current, the concentration of solar light on highly efficient PV cells has been proposed several decades ago as a possible means to reduce the cost of PV energy. Concentration of solar light by a factor (C) of, e.g., 10 or 100, could theoretically reduce the price of the produced electrical energy by the same ratio but the additional costs associated with the concentration system limit the actual cost-cutting. The potential advantages of solar light concentration depend on the characteristics of incident light (direct or diffuse), on the behavior of PV cells under concentrated light, and on the possibility to fabricate cost-effective concentration systems. Classical imaging concentration systems are based on the reflection and/or refraction of light. Parabolic mirrors can lead to high C values but the need to position the PV cells above the reflecting surface makes their encapsulation and cooling difficult. Fresnel lenses are less sensitive to defects of fabrication and sun tracking errors than parabolic mirrors and can lead to C values up to ≈50. However, their limited angular field implies their association with expensive sun-tracking systems. The luminescent solar concentrator (LSC) introduced at the end of the 1970s is a nonimaging concentration system that resorts to a quite different concept. An LSC consists of a plate of a transparent material of high refractive index containing luminophores capable to absorb a large fraction of the solar spectrum and to reemit the absorbed light at longer wavelengths through photoluminescence (PL) processes (**Figure 1**). Thanks to the high refraction index of the host matrix, a large fraction of the emitted photons is trapped within the plate and guided by total internal reflections (TIRs) to part or totality of the perimeter where highly efficient PV cells convert the collected light into electrical energy.[1–4] An LCS, thus, possesses the double function of conversion of the absorbed light into photons of longer wavelengths through PL processes and of concentration of the trapped emitted light by the waveguide constituted by the host matrix.

Compared to classical imaging concentration systems, LCSs present several potential advantages. Because of the low angular dependence on the direction of the incident light, they do not require sun-tracking system. LCSs operate efficiently under diffuse light, which is of particular interest for countries with frequent cloudy weather.[5] Furthermore, thanks to the absorption/emission associated with PL processes, hot photons generally deactivated through thermal processes in PV cells can be converted into longer wavelengths, thus limiting

Prof. J. Roncali
Supramolecular Organic and Organometallic Chemistry Center
Babes-Bolyai University
11 Arany Janos str., Cluj-Napoca 400028, Romania
E-mail: jeanroncali@gmail.com
Prof. J. Roncali
Moltech Anjou CNRS
University of Angers
2Bd Lavoisier, Angers 49045, France
The ORCID identification number(s) for the author(s) of this article can be found under https://doi.org/10.1002/aenm.202001907.

DOI: 10.1002/aenm.202001907

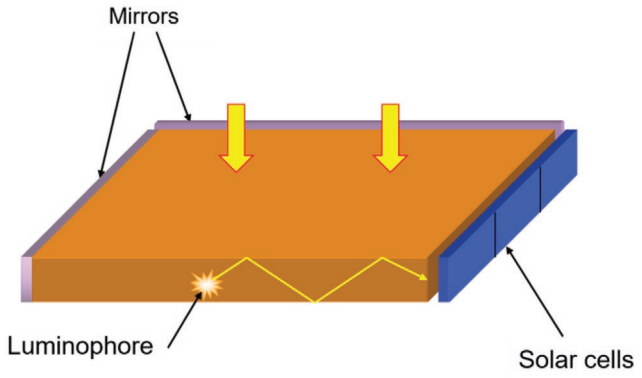

Figure 1. Luminescent solar concentrator.

the problems related to the dissipation of thermal energy in the PV cell. Finally, the possible large variety of color, shape, and degree of transparency of LSCs clearly represents aesthetically appealing advantages for the building integration of PV energy (BIPV) in modern urban environment.[6,7] Proposed at the end of the 1970s for solar application,[1–4] LCSs have been intensively investigated in the United States and Europe during the 1975–1985 decade. However, at the end of the 1980s, interest in these devices rapidly declined. This can be explained by a conjunction of intrinsic factors such as insufficient performances and stability of LSCs, and extrinsic causes such as the decrease of the price of oil after the 1973 and 1979 crises and the dramatic reduction of the price of silicon PV cells that made the concentration of solar light less attractive (**Figure 2**).

After some 20 years of silence, a renewal of interest for LSCs started in the first years of the millennium, resulting in a rapid increase and the number of publications (**Figure 3**).

However, this renaissance takes place in a completely different economic, environmental, and scientific context and recent developments of the field seem to obey to different motivations. Although the reduction of the cost of PV energy by concentration of solar light is still invoked in the majority

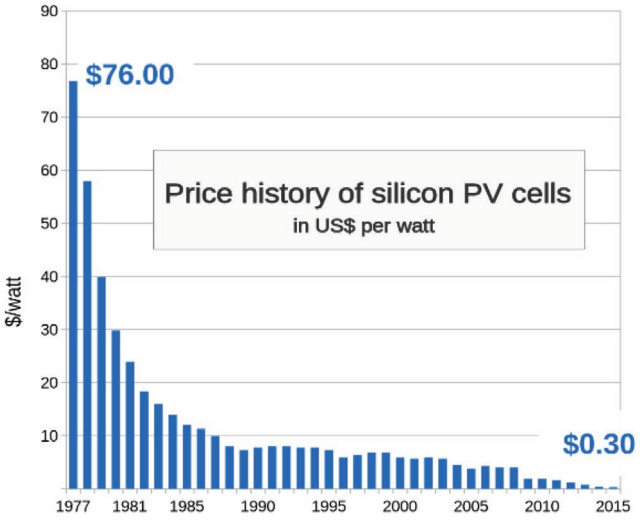

Figure 2. Evolution of the price of silicon solar cells (data source: Bloomberg New Energy Finance and pv.energy.com).

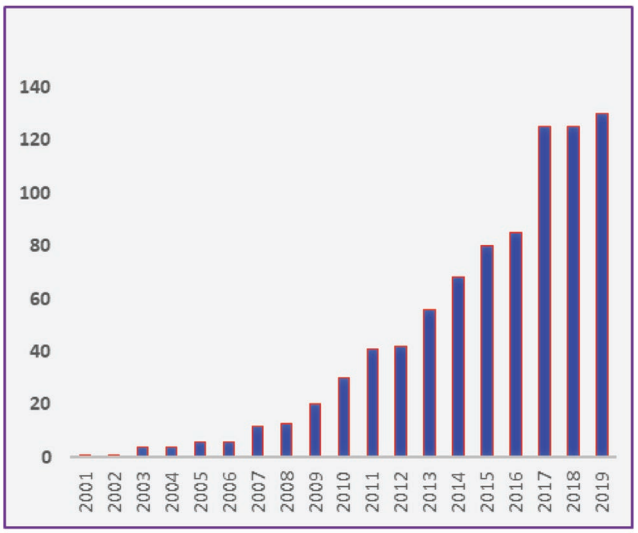

Figure 3. Annual number of publications on LSCs (source: Web of Science).

of publications, examination of recent literature clearly shows that light concentration is obviously no longer the main objective and that research now essentially focuses on the development of light conversion systems for BIPV without necessarily implying light concentration.

LSCs have been subject to previous reviews.[6,9,10] However, the continuing interest in the field attested by the increasing number of publications, the recent developments of new generations of emitting materials, the emergence of novel applications as well as some persistent confusion regarding the definition and characterization of the performances of LSCs underline the potential interest of an updated critical review on this topic. After a brief historical and a general presentation of the operation principles and characterization of LSCs, an overview of the host matrix and emitting materials, the various technological approaches of device fabrication and the applications of LSCs will be presented. Finally, the performances of LSCs will be critically discussed on the basis on experimental results obtained on real devices with particular emphasis on the question of efficiency versus concentration factor that remains a source of confusion and a major problem for real applications.

2. Historical Background

In 1949, Shurcliff and Jones published some first ideas on radiance amplification with luminescent systems.[11,12] In 1970, inspired by these ideas, Kiel developed this concept in the case of scintillators and discussed some basic aspects such as the shape of the system, the role of reflectors, the function of the emitter, the major problem of reabsorption of luminescence, and reported some first experimental results.[8] In 1976, Weber and Lambe published their seminal article "Luminescent Solar Collector for Solar Radiation" in which reference to solar energy appears for the first time with the idea of reducing the cost of PV electricity by concentration of solar light on solar cells.[1] In a following article, Levitt and Weber discussed one of the major alternatives for the fabrication of LSCs, namely

polymer matrixes and organic dyes versus glasses doped with inorganic luminophores.[13] At the same time, Goetzberger et al. proposed multi-stack LSCs combined with solar cells based on different semiconductors (Si, GaAs, Ge) and discussed thermal energy conversion with LSCs and their operation under diffuse light.[2,5,14] In 1977, Zewail and co-workers reported a first example of multi-dye LSC based on Förster resonant energy transfer (FRET)[3] and in 1979, they published a detailed theoretical analysis of LSCs pointing out the effects of self-absorption (SA) in relation with chromophore dipole orientation for both absorption and emission processes and reported some first results on the stability of dyes upon operation.[15] LSCs based on uranyl-doped glasses were proposed by Reisfeld in 1978.[4,16] Yablonovitch discussed the thermodynamics of LSCs and the relationships between the optimal concentration factor and the Stokes shift of the emitter.[17] In the following years, several experimental investigations have been published. Batchelder and Zewail analyzed LSCs based on a large series of laser dyes and investigated both liquid and bulk prototypes.[18] Olson et al.[19] and Sanregret et al.[20] discussed the problem of reabsorption of luminescence and proposed a system based on radiationless excitation transport with excimer-forming chromophores. Thomas et al. investigated matrix losses,[21] and Heidler described in detail an experimental setup for the characterization of relatively large-sized LSCs (400 cm^2) and investigated LSCs based on ten different dyes.[22] Drake et al. fabricated multi-stack square collectors of 10 and 30 cm. They pointed out the increase of optical efficiency when reducing the size of the collector and reported an optical efficiency of 7.5% for a single-dye device.[23] Friedman discusses various configurations of LSCs including uniformly doped bulk devices, thin-film, stacked, and multilayered LSCs and described a device with an electrical efficiency of 3.2%.[24] Liquid LSCs were investigated in particular by Valeur and co-workers in 1982[25] and shortly after by Lifante et al. who also reported one of the first examples of bottom cell LSC.[26] The effects of the geometry of the collector were analyzed by Roncali and Garnier in 1984 and Loh and Scalapino in 1986.[27,28] The effects of diffusing back reflectors were investigated by several groups[23,26,27,29,30] while thin-film LSCs consisting of an heavily doped thin film deposited on the surface of a transparent waveguide were also introduced during this early period.[18,24,31] This short historical survey shows that the major concepts, problems, and technical aspects of LSCs that are still subject to intensive research effort today were already identified, discussed, and experimentally investigated in early works.

3. Working Principles of LCSs

The most evident feature of an LSC is its geometric factor or geometric gain (G) defined by the ratio of the area of the input surface (A_{in}) to the area of the edge where the concentrated emitted light is collected (A_{out}) (Equation (1))

$$G = A_{in}/A_{out} \tag{1}$$

G represents the theoretical limit of the concentration factor C that can be defined either by the ratio of the flux of collected photons (N_{out}) to the number of incident photons (N_{in})

$$C_n = N_{out}/N_{in} \tag{2}$$

or by the ratio of the output emittance (P_{out}) to the input irradiance (P_{in})

$$C_p = P_{out}/P_{in} \tag{3}$$

The limit of C_p is determined by the energy loss associated with the conversion of the absorbed light by the PL process (Stokes shift), the energy lost in this conversion being thermally dissipated.[17]

In view of Equations (1)–(3), one may expect C to increase linearly with G. However, since the operation of an LSC is associated with multiple loss factors, C follows a sub-linear dependence on G and reaches an asymptotic value determined by the characteristics of the emitter and of the host matrix. C is, thus, a measure of the optical efficiency of the LSC (η_{opt}) defined by Equation (4)

$$\eta_{opt} = C_n/G \tag{4}$$

While the energetic efficiency η_{en} is given by Equation (5)

$$\eta_{en} = C_p/G \tag{5}$$

C_n and η_{opt} quantify the purely optical functions of an LSC that involve the absorption, conversion, transport, and concentration of solar light. If the LSC is considered a particular kind of PV generator, the characteristics of the attached PV cells must be taken into account in order to define the electrical efficiency (η_{el}) of the whole system (Equation (6))

$$\eta_{el} = \eta_{opt} \times \mathrm{PCE} \tag{6}$$

where PCE is the power conversion efficiency of the PV cell defined by the product of the short-circuit current density (J_{sc}), open-circuit voltage (V_{oc}), and fill factor (FF) divided by the incident light power (P_{in}). Using the input surface of the LSC A_{in} as reference gives the PCE of the LSC-PV cell generator

$$\mathrm{PCE} = J_{sc} \times V_{oc} \times \mathrm{FF}/P_{in} \tag{7}$$

Although this quantity is frequently used in recent literature, it presents the inconvenience of occulting the optical efficiency of the LSC as well as the concentration factor. While less frequently reported, it is also interesting to characterize the external quantum efficiency (EQE) of the system defined as the ratio of the number of charges generated by the PV cell to the number of incident photons on the LSC under monochromatic illumination.

The optical and electrical efficiencies of a LCS can be also expressed by the product of the partial efficiencies associated with the individual processes involved in the operation. These various factors can be roughly divided into three main categories associated with different functions of an LSC, namely the absorption of solar light, its conversion into photons of longer wavelengths, and their transport (with eventual concentration) to the output edge(s). The conversion of the output light by PV cells represents a fourth process that is not an intrinsic

characteristic of the LSC since it depends on the PCE and spectral response of the PV cells. To these various elemental mechanisms are associated specific loss factors.

3.1. Reflection on the LSC Surface

The reflection of part of the incident light by the surface of the LCS represents a first loss factor. For a normal incidence, the fraction of reflected light L_r is given by Equation (8) where n is the refractive index of the matrix

$$L_r = (n-1)^2/(n+1)^2 \tag{8}$$

For n = 1.5, a typical value for polymethyl methacrylate (PMMA) or glass matrixes, $L_r \approx 4\%$, and the fraction of light penetrating the LSC η_{pen}

$$\eta_{pen} = 1 - L_r = 4n/(n+1)^2 \tag{9}$$

While normal incidence is the only case considered here, it is clear that in real conditions, light reflection for all incidences should be considered.[15]

3.2. Trapping Efficiency

After absorption and re-emission by the luminophore, a fraction of the emitted light remains trapped in the LCS while a substantial part is lost. For an isotropic emission, only photons emitted with an angle inferior to a critical value (θ_c) remain trapped in the matrix by TIR. According to Descartes–Snell's law, θ_c is related to n by

$$\theta_c = \sin^{-1}(1/n) \tag{10}$$

In a 3D space, θ_c generates a loss cone and all photons emitted within the solid angle generated by θ_c will escape the device. The light lost through the two boundary planes of the LSC (L_c) is given by

$$L_c = 1 - \left[(n^2-1)^{1/2}/n\right] \tag{11}$$

and the trapping efficiency (η_{trap}) is

$$\eta_{trap} = (n^2-1)^{1/2}/n \tag{12}$$

For a typical n value of 1.5, ≈25% of the emitted light is lost and $\eta_{trap} \approx 0.75$. Although an increase of n improves η_{trap}, it also increases the reflection losses, and the product $\eta_{pen} \times \eta_{trap}$ that represents ≈72% of the incident light for n = 1.5 admits a broad maximum of ≈77% for n = 1.8–2.0.

3.3. Light Absorption

Neglecting the absorption by the host matrix, the number of photons ($N_{(\lambda)}$) absorbed by the luminophore at a given wavelength λ depends on the absorption coefficient of the emitter $\alpha_{(\lambda)}$ (defined by the product of molecular absorption coefficient of the emitter by its concentration in the matrix) and the thickness d of the LSC according to the Beer–Lambert law

$$N_{(\lambda)} = N_{0(\lambda)}(1 - 10^{-\alpha(\lambda)d}) \tag{13}$$

the number of photons absorbed from the solar spectrum (η_{abs}) being

$$\eta_{abs} = \int N_{(\lambda)} d\lambda \tag{14}$$

3.4. PL Quantum Yield of the Emitter

If the PL efficiency of the luminophore (ϕ_{PL}) is inferior to unity as in most cases, ϕ_{PL} determines a third loss factor (η_{PL}). The product of these four factors determines the conversion efficiency of the LSC (η_{conv}), namely the theoretical number of emitted photons available for light-guiding

$$\eta_{conv} = \eta_{pen} \times \eta_{abs} \times \eta_{trap} \times \eta_{PL} \tag{15}$$

3.5. Total Internal Reflection

The photons emitted within the matrix are transported to the output edge by TIRs. An optimal waveguiding function of an LSC implies perfect boundary surfaces. However, in the real world, the rugosity of the surfaces, surface defects, dust, scattering centers, or local variations of refractive index result in a non-unity effective TIR coefficient R_{TIR}. Although R_{TIR} = 1 is postulated in many theoretical models, the actual waveguiding function of an LSC is affected by a loss factor (η_{TIR}) that depends on R_{TIR} and on the average number of internal reflections (n_r) (Equation (16))

$$\eta_{TIR} = R_{TIR}^{nr} \tag{16}$$

3.6. Lateral Reflections

When striking the side edges of the LSC, the emitted photons are also subject to TIR, and hence to critical cone losses. Whereas the collection of photons at the output edge equipped with PV cells must be optimized, in contrast, the escape of photons through the other sides of a polygonal LSC must be blocked by reflective coatings such as metal mirrors or diffusing white coatings. The reflection coefficient of these lateral mirrors (R_s) as well as the number of reflection on these side mirrors (n_s) determine a loss factor (η_s) given by

$$\eta_s = R_s^{ns} \tag{17}$$

3.7. Reabsorption of PL by the Host Matrix

The material used as host matrix for LSCs generally presents a good optical transparency in the practical spectral range, and thus reabsorption of luminescence by the matrix is often

considered negligible. While this assumption is valid for small devices, for large-area LCS, the absorption by the matrix can become significant.[31] This absorption leads to a loss factor given by

$$\eta_{\text{host}} = N_{0(\lambda)}(1-10^{-\alpha L}) \quad (18)$$

where $\alpha_{(\lambda)}$ is the absorption coefficient of the matrix and L is the distance traveled by the photons.

3.8. Self-Absorption of PL by the Emitter

The reabsorption of the emitted light the luminophore itself probably represents one of the major limitations to the efficiency of LCSs. This problem (discussed in detail in the next part) was identified at an early stage,[1,8,15,18–27] and continues to give rise to an abundant literature. This reabsorption process determines a partial efficiency $\eta_{\text{self.}}$

3.9. Stokes Shift

The absorption of photons and their re-emission at a longer wavelength is accompanied by an energy loss and an associated partial efficiency (η_{Stokes}). Because of the red shift associated with SA, a correct evaluation of η_{Stokes} should take into account the Stokes shift effectively observed at the LSC output (which depends on the optical path length, and hence on the size of the LSC) and not that observed on PL spectra recorded in diluted solutions. As discussed below, the difference can be very large, up to several tenths of nanometers. Note that besides an energy loss, the red shift of the emission spectrum exerts also a positive effect by providing to the PV cell an excitation spectrum closer to its spectral range of optimal efficiency. At this stage, the optical efficiency of an LSC (η_{opt}) is determined by the product of the partial efficiency of nine elemental processes

$$\eta_{\text{opt}} = \eta_{\text{pen}} \times \eta_{\text{abs}} \times \eta_{\text{trap}} \times \eta_{\text{PL}} \times \eta_{\text{TIR}} \times \eta_{\text{host}} \times \eta_{\text{LR}} \times \eta_{\text{self}} \times \eta_{\text{Stokes}} \quad (19)$$

3.10. Coupling with PV Cells

The last step consists of the collection of the emitted photons reaching the output of the LSC and their conversion into electrical energy. When these photons hit the output diopter, only 12.5% of them leave the LSC through the loss cone while the rest is reflected back by TIR. If all but the output edges are equipped with mirrors, these photons are guided back towards the output edge with again a 0.125 probability to leave the LSC through the loss cones. Consequently, ≈20 TIR reflections on the output edge are required to collect ≈95% of the emitted photons ($1–0.875^{20}$). In fact, this is only hypothetic since the reflected photons travel longer distances and undergo again the various losses associated with transport. Therefore, connecting a PV cell to the output edge by an air gap, as reported in several publications, is clearly inappropriate. In contrast, an index-matching material with refractive index higher than that of the matrix is needed to collect a maximum amount of emitted light. This imperfect coupling process can, thus, result in another loss factor. At this final stage, the electrical efficiency (η_{el}) of the whole system is defined by the product of the optical efficiency of the LSC and PCE of the PV cell (Equation (7)) (in the spectral range corresponding emission spectrum of the LSC ($\Delta\lambda$).

The modelization of LSCs has been developed in numerous publications.[33–46] Some of them are essentially focused on the thermodynamics aspects of light conversion,[33–40] while other loss factors and in particular SA or recent technical developments such as photonic band filters or chromophore orientation have been also considered with the aid of ray-tracing programs and Monte-Carlo methods.[41,42] In many cases, modelization focuses on some particular factors while some others are neglected, for example, matrix absorption, or assumed to be quantitative, for instance TIR or ϕ_{PL}. Many models appears excessively idealized and lead to over-optimistic predicted performances. Besides a high degree of redundancy, a recurrent problem is that many of these models are experimentally "validated" with results obtained on very small devices for which, in addition to some bias, some loss factors that significantly impact the performances of large-scale LSCs are negligible for miniature devices. A consequence of these various problems is that many idealized models lead to predicted limits of the concentration factor several orders of magnitude higher than the best reported experimental results.[46]

4. Characterization of LCS

Although some authors recommend to treat an LSC as any PV device.[47] It should be emphasized that an LSC is before all an optical system that should be characterized as such before any association with PV cells. Furthermore, as illustrated in some recent work, PV conversion is not the exclusive application of LSCs. Besides the determination of the optical and/or electrical efficiency by measuring the in/out balance of the photon flux or luminous power, the full characterization of an LSC requires a number of measurements on both the emitter and the matrix. Some of them are simple routine but some others require more complex experimental procedures. For usual matrix materials, e.g., glass or PMMA, the optical characteristics, namely the refractive index and the light absorption and hence the factors η_{pen}, η_{trap}, and η_{host}, are known. However, when less conventional host materials are used, the refractive index and absorption spectrum over the spectral range extending from the short wavelength absorption onset of the emitter to the long wavelength limit of the PV cells response must be determined. The PL emission characteristics of the emitter in solution are easily obtained, but once imbedded in the rigid environment of the host matrix, ϕ_{PL} is influenced by various factors such as concentration, dielectric constant of the matrix, refractive index, conditions of polymerization, and additives, and therefore should be determined under these specific conditions.[18,20,23,35,48,49]

The losses associated with the matrix absorption are often considered as negligible, which is a reasonable assumption for small devices; however, the situation is different as the size of the LSC approaches that of real utilization, for example, windows. Experiments on PMMA fibers have shown that at the He–Ne laser wavelength (632 nm), absorption by the sixth

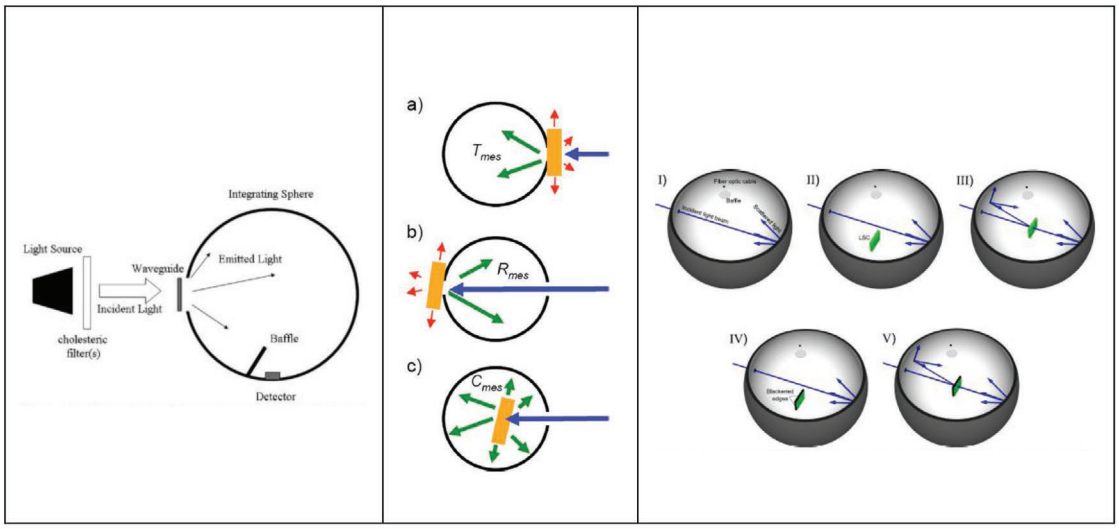

Figure 4. Characterization of LSCs with integrating spheres. Left: measurements of surface losses, the edge emission was measured in the same way on horizontal sample vertically illuminated. Reproduced with permission.[50] Copyright 2008, The Optical Society of America. Middle: determination of the spectral collection efficiency of an LSC; a,b) reflection and transmission measurements; c) total emission measurement. Reproduced with permission.[51] Copyright 2009, American Institute of Physics. Right: determination of the internal optical efficiency and loss channels of an LSC: I) empty integrating sphere; II) LSC inside the sphere but not directly illuminated; III) LSC illuminated by the incident light beam; IV) same as (III) but the side surfaces are blackened; (V) same as (III) but the side surfaces are blackened. Reproduced with permission.[52] Copyright 2016, Elsevier.

harmonic of the C—H stretch vibration can lead to a loss as large as 0.4 cm^{-1}.[32] Partial fluorination of the polymer structure can be expected to contribute to solve this problem.[7] Due to surface defects, scattering centers, dust, or local variations of refractive index, TIR is in fact associated with an apparent coefficient of reflection. For example, a value of 0.997 ± 0.03 was measured by multiple internal reflections of a laser beam on a 100 cm long PMMA plate of common optical quality.[27] Thus, for an average number of internal reflections of 50, (a plausible value for a 100 cm optical path), $\eta_{TIR} = 0.86$, which is not negligible. However, these transport losses as well as those directly related to the loss cone are subject to large variations depending on the nature, concentration, overlap of the absorption and emission spectra, and PL quantum yield of the emitter. The number of photons lost through the two boundary sides of LSCs has been quantified by various sequences of measurements with integrating spheres (**Figure 4**). A typical series of experiments involve measurement of the light emitted by the top surface under front excitation, by the bottom surface under transmitted excitation, and by all of the LSC surfaces and perimeter. An alternative method consists in measuring the total emission before and after the perimeter or the top and bottom surfaces have been blackened (**Figure 5**). Debije et al. reported that 40–50% of emitted photons are lost through the top and bottom surfaces, a quantity that largely exceeds the 25% generally admitted for a common refractive index of 1.5.[50] In fact, in addition to the refractive index, the escape of photons through the boundary surfaces is tightly imbricated with the phenomenon of SA and re-emission, and, thus, depends also on ϕ_{PL}. While other authors obtained slightly lower values,[51,52] there is a large agreement on the fact that in doped LSCs, the losses calculated on the sole basis of the refractive index are underestimated.

4.1. Self-Absorption and Stokes Shift

Most of the luminophores present an overlap of their absorption and emission bands that results in the reabsorption of a more or less important fraction of the emitted light by the luminophore itself. Since this SA process essentially affects the shorter wavelength region of the emission band, the PL spectrum observed at the output of an LSC exhibits a progressive bathochromic shift as the distance traveled by the photons increases. SA is one of the major limitations to the efficiency of LSCs but constitutes also a driving force for research since a huge effort is focused on the development of new emitters with

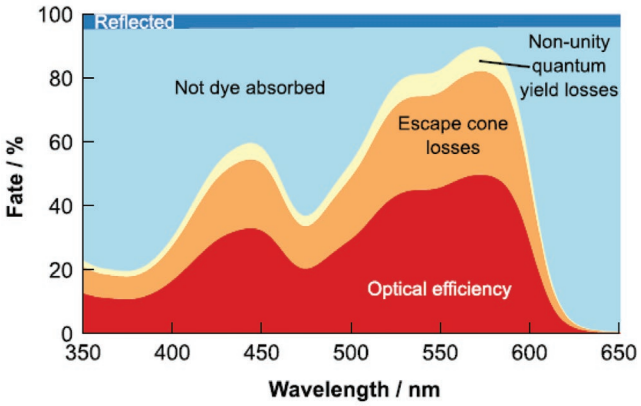

Figure 5. Spectral dependence of the fate of photons relative to the number of incident photons on an LSC doped with lumogen 305. Photons are reflected off by the top (blue), not absorbed (light blue), lost due to non-unity ϕ_{PL} (yellow), lost via the escape cone (orange), or guided towards the output surface (red). Reproduced with permission.[52] Copyright 2016, AIP Publishing.

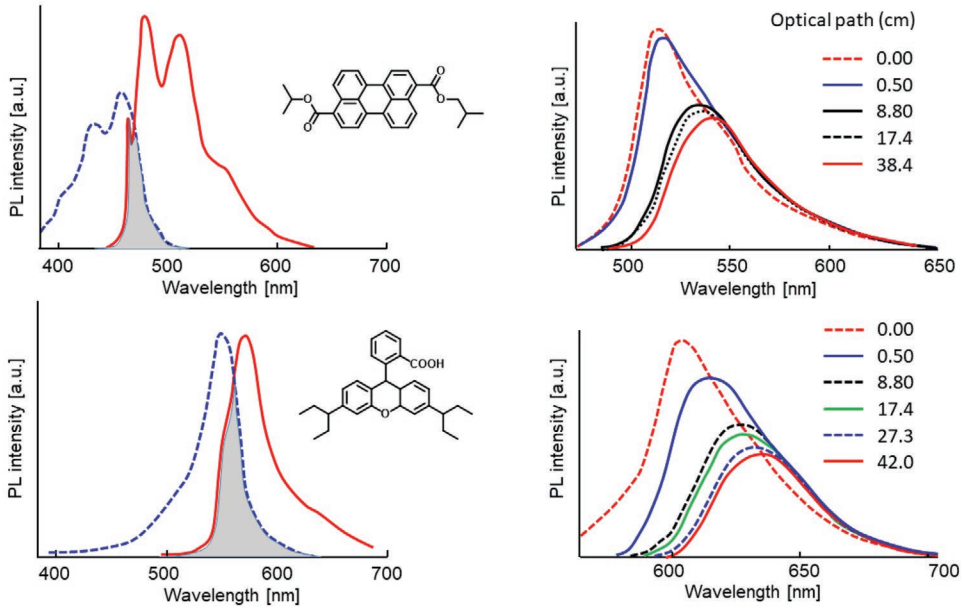

Figure 6. Left: absorption and PL emission spectra of a solvent green 5 (top) and rhodamine B (bottom). Right: PL emission spectra collected at the output of the corresponding LSCs of increasing optical paths (in centimeters). Input areas 50–400 cm^2. Adapted with permission.[27] Copyright 1984, The Optical Society of America.

reduced SA. The analysis of SA is a complex problem since its magnitude is determined by the overlap of the absorption and emission spectra of the emitter, its absorption coefficient, concentration, ϕ_{PL}, and Stokes shift on one hand, and by the refractive index, thickness, η_{TIR}, η_{Lat}, and eventual scattering centers on the other hand. The possibility of multiple reabsorption re-emission events leads to a complex and variable intrication of these various parameters.[15] SA was identified long ago as secondary emission effect for fluorescence in solutions and for this reason, low absorbance is recommended for accurate determination of ϕ_{PL}.[53,54] Since the beginning of research on LSCs, SA has been a matter of intensive theoretical and experimental work. Already in 1970, Keil investigated polymer matrixes doped with fluorescent dyes and observed a strong decrease of luminescence in the first 20–50 mm of the optical path followed by a slow exponential decay up to the maximum distance of his experiments (40 cm).[8] A common method to evaluate SA is based on the ratio of the integrated emission spectrum at the output of an LSC to that of an assumed SA-free spectrum recorded in dilute solution or by front illumination of the LSC. Recording output emission of an LSC illuminated by a small light spot located at an increasing distance from the output is routinely used in the LSC literature to evaluate SA. A related method consists of recording the PL spectrum at the output of fully illuminated LSCs of increasing dimensions corresponding to increasing optical path lengths. This method presents the advantage to give the emission spectrum effectively seen by the PV cells when the LSC is fully illuminated (**Figure 6**).[27] However, in both cases, the observed output emission spectrum is not exclusively affected by SA but also by other transport-dependent losses in particular scattering and cone losses. SA is a problem common to almost all classes of emitters and depends not only on the Stokes shift but mostly on the overlap of absorption and emission spectra and in particular on the existence a long absorption tail. SA is discussed in most of the publications on LSCs, and with the renaissance of research on LSCs, SA has given rise to many theoretical and experimental studies on new organic and inorganic emitters.[13,18–20,23,25,27,55–57,59–61]

4.2. Efficiency of LSCs

When considered as a light converter and concentrating system, the optical efficiency of an LSC is defined by the product of the elemental partial efficiencies of Equation (16). As a PV generator, an LSC is characterized by the product of the V_{oc}, J_{sc}, and FF of the PV cells, divided by the power of the light incident to the LSC input surface. This ratio represents the PCE of the system sometimes quoted as the electrical efficiency (η_{el}). Since PCE depends on the efficiency of the PV cell at the emission wavelength of the LSC, the same device can show large variations of PCE with PV cells of different spectral responses (**Figure 7**). GaAs cells give generally higher values.[27,31,62,64] Consequently, PCE is poorly informative regarding the optical performances of an LSC. The optical efficiency is defined either by the ratio of the in/out photon flux or luminous power, giving, respectively, η_{opt} and η_{en}. These two quantities differ by the energy loss associated with the Stokes shift. Although the intrinsic values of η_{opt} and C are certainly the most relevant parameters, their accurate experimental determination is not straightforward and an integrating sphere is needed to establish a complete optical balance of LSCs and determine η_{opt} through a series of experiments,[50–52,65,66] but the use of this method is essentially limited to small samples. The concentration factor C is often assimilated to the ratio of the current produced by a cell attached at the LSC output to that of a similar cell facing the excitation light while η_{opt} is obtained

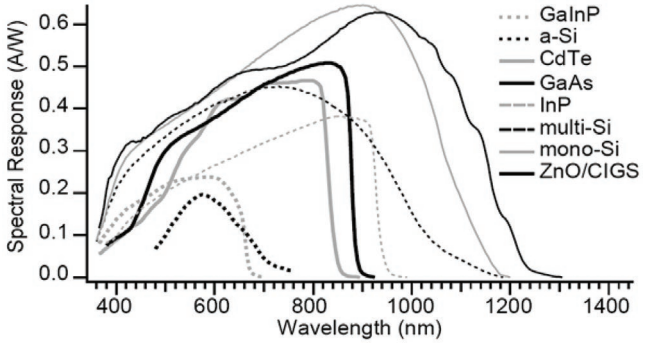

Figure 7. Spectral response of different types of PV cells.

by the product $\eta_{opt} = C \times G$. This method has the advantage of simplicity since only two PV cells are necessary. However, the obtained values are not rigorously exact since they depend on the spectral response of the PV cell and on the quality of the optical coupling between the LSC and the PV cell. Due to a narrower spectral response (Figure 7), GaAs cells give generally higher η_{opt} and C values than silicon cells with luminophores emitting in the visible region.[27,31,62] With these provisions in mind, this method gives a good estimation of the optical performances of an LSC and it is very convenient for investigating homogeneous series of devices based on the same emitter. Furthermore, it has the advantage to be close to the real conditions of operation of LSCs.

In many cases, the PV cells cover only a portion of the output surface while the rest of the perimeter is provided either with mirrors to increase G, or by black absorbing layers, assuming that the whole output surface or perimeter give a PL intensity equal to that observed at the measuring point. However, higher luminous intensities are generally observed in the middle of the output edge[22,63] and a full coverage of the whole perimeter is clearly the best option. The literature reveals also a large variety of conditions of illumination with various type of light sources such a mercury[4,13] or Xenon lamp,[18,22,27] outdoor solar illumination,[23,26] or even indoor with cloudy weather,[64] but the use of solar simulators with standard AM 1.5 conditions tends to generalize. Several groups have used integrating spheres in order to establish a complete optical balance of LSCs and determine η_{opt} through a series of experiments.[50–52,65,66] However, the use of this technique is limited to small devices. Finally, the characterization of LSC also suffers from the absence of universally adopted definitions of the relevant parameters, i.e., geometric gain, concentration factor, and optical efficiency and of standard conditions of measurement. Besides AM 1.5 simulated solar light, C and η_{opt} are sometimes calculated by integration of the EQE spectrum obtained with partial illumination of the device,[65] by reference to the fraction of light absorbed by the LSC[67] or measured under illumination restricted to the absorption band of the emitter.[68] C and η_{opt} have been also calculated by comparison with non-doped matrixes. This leads to C values >1 while when referred to the incident light C is largely inferior to unity.[69] Some authors have used their own definition of G that is not considered as an intrinsic property of the LSC but depends on the size of an illuminated zone or of an aperture at the output of the device.[70,71] Although these specific experimental conditions and definitions can be useful for discussing some fundamental aspects, it is clear that the use of home-made definitions of performances parameters contributes to the large confusion existing on these questions. It took several years before the field of organic solar cells finally adopted standard definitions of PCE, EQE, and conditions of illumination. With an increasing research activity on LSCs, the standardization of definitions, conditions of measurement, and requirements regarding data reporting becomes urgent because the continuation of the present highly confusing situation may cast some doubt on the validity of the research on LSCs and more generally on the credibility of the topic.

5. LSCs Components

5.1. Host Matrix Materials

Although a few examples of liquid LSCs have been reported, the vast majority of devices are made of solid materials such as glasses and polymers. The role of the host matrix in general or of polymer matrixes in LSCs has been discussed in two recent reviews.[72,73]

5.1.1. Liquid LSCs

Liquid systems present the advantages of easy modification of device geometry and concentration of luminophores and easy replacement of the emitting solution after photo-degradation. Liquid LSCs were initially investigated by Valeur and co-workers. Aluminum mirrors disposed vertically in a 20 × 20 cm tank allowed to realize LCSs of various geometries with G values varying from 5 to 40. DMSO was used as solvent due to its high refractive index. Most of devices gave $C < 1$ except for that with the highest G of 40 for which C was 1.21.[25] Lifante et al. reported a C of 1.30 for a liquid LSC in which the PV cells were placed at the bottom of a recipient containing a fluorescent solution.[26] The same group also reported outdoor evaluation of liquid LSCs.[74] Mansour analyzed liquid LSCs with G of 2.8 containing three different dyes in Triton X-100 and reported optical efficiencies of ≈20% (corresponding to $C = 0.55$). By comparing with bulk PMMA devices of 5 × 10 × 0.28 cm ($G = 3.5$), it was concluded that both systems are equivalent.[75] More recently, liquid LSCs were used to compare various classes of emitters including dyes, conjugated polymers, and quantum dots (QDs). Optical efficiencies ranging from 0.30% to 3.4% were reported, organic dyes leading to the best results.[76] Emitting materials based on phycobilisomes have been evaluated in water-based devices.[77] Liquid LSCs were used to evaluate PbS QDs emitters or to investigate FRET in functionalized QDs.[78,79] Circular liquid LSCs equipped with silver PV cells have been reported.[80] In an attempt to mitigate SA, Krumer et al. analyzed an LSC based on a highly concentrated Lumogen Red 305 in toluene and reported a C of 1.5 for a 3.5 × 10 cm system ($G = 10$).[81] Very recently, Rosei and co-workers reported liquid LCSs containing "eco-friendly" Cu-doped ZnInSe QDs dispersed in toluene or embedded in a polymer matrix. An optical efficiency higher that 3.5% was reported for a G = 15

device ($C = 0.45$), a value twice larger than that obtained with a bulk polymer device with $G = 10$.[82]

5.1.2. Glass LSCs

LSCs based on glasses doped with inorganic emitters have been initially proposed at the end of the 1970s and investigated then by several groups.[4,13,83–85] Reisfeld et al. reported a C of 1.50 for an LSC of unspecified dimensions doped with uranyl ions under irradiation with a mercury lamp.[4] Later on, they proposed to take advantage of energy transfer between neodymium, uranyl, and holmium ions to improve the absorption of the solar spectrum, and, thus, the collection efficiency of LSCs.[16] In 1983, the same group investigated Vycor porous glass impregnated with metal complexes to fabricate LSCs, but the performances of such systems were not evaluated.[83] The weight and limited possibilities of doping, in particular with organic dyes, have restricted the use of glass matrixes. However, as discussed below, glass is still widely used as transparent substrate for thin-film LSCs.

5.1.3. Polymer-Based LSCs

Since early work on LSCs, acrylic polymers, and, in particular, PMMA have been the most widely employed host materials due to their good optical and mechanical properties and relatively high refractive index. Thomas et al. investigated the role of matrix losses experimentally and theoretically and concluded that scattering and TIR were the dominant loss factors while SA was not an inherent limitation to high-concentration factors.[21] More recently, motivated by the effect of the dielectric constant on the Stokes shift, Reda investigated the changes in the electric and dielectric properties of PMMA upon doping with dyes.[86] Kastelijn et al. reported a comparative study of small size thin-film LSC (5 × 5 cm) based on quartz, polycarbonate, and PMMA and found no significant difference on the performances of the resulting LSCs; however, this conclusion is questionable in view of the small size of the devices.[87] Fattori et al. reported that low molecular weight poly(lactic acid) films chemically modified or blended with an oligothiophene luminescent dye combine excellent processability and photostability while the same dye shows a higher ϕ_{PL} than in PMMA.[88] El Bashir reported that the introduction of SiO_2 nanoparticles in a PMMA matrix doped with a coumarin dye leads to an improvement of the trapping efficiency of thin films.[89] Unsaturated polyesters (UPs) mixed with methyl methacrylate have been proposed as an alternative to PMMA matrixes and it was reported that the refractive index of UPs, already higher than that of PMMA, could be increased up to 1.585 upon addition of 5% MMA.[90] Melucci et al. proposed water-soluble silk fibroin as possible matrix material for LSCs and investigated the PL of an incorporated bio-modified luminophore.[91] Griffini et al. synthesized a new host matrix system by cross-linking a functional chloro-trifluoro-ethylene-vinyl-ether copolymer with an aliphatic isocyanurate cross-linker. LCSs based on this matrix showed performances comparable to those of PMMA based systems ($\eta_{opt} \approx 2.5$–2.8%) but presented a better long-term stability.[92,93] Films of dye-doped parylene have been prepared by co-evaporation of parylene and dye under vacuum. Thin-film LSCs (5 × 5 × 0.5 cm, $G = 2.5$) were fabricated by deposition on a high refractive index glass substrate ($n = 1.805$ at 588 nm), a η_{opt} of 7.2% was obtained with a GaAs cell raising to 22.6 when a white diffuser was placed behind the LSC, leading in this case to a $C = 0.57$.[94] Thin-film LSCs of 5 × 5 × 0.3 cm were prepared by casting an epoxy resin doped with coumarin 6 on glass substrates. Improved C and η_{opt} values compared to those obtained with PMMA thin films were reported ($C = 1.23$ vs 1.13 and $\eta_{opt} = 7.4\%$ vs 6.7%).[95] Very recently, Tatsi et al. described a first example of thin-film LSC based on a thermally reversible cross-linked host polymer capable of self-healing upon thermal treatment. A prototype doped with a perylene-based luminophore gave a η_{opt} of 4.9% while it was shown that a damaged device undergoes full recovery of efficiency after complete thermal healing.[96]

5.1.4. Flexible LSCs

The possibility to develop flexible LSCs has emerged recently. Buffa et al. use polysiloxane rubber waveguides doped with different concentrations of Lumogen Red 305. The results obtained with GaAs and silicon PV cells led to the conclusion that there was no significant difference between polydimethylsiloxane (PDMS) and polycarbonate waveguides.[97] LSCs based on PDMS matrixes doped with coumarin 440 and disodium fluorescein have been fabricated. A 5 × 5 × 0.5 cm device ($G = 2.5$) with a TiO_2 bottom layer gave a $\eta_{opt} = 29\%$ ($C = 0.73$) and PCE of 4.62%.[98] In a following article, the same group reported a η_{opt} of 42% with $C = 1.05$ and a certified PCE of 5.57%.[99] Correia et al. investigated flexible LSCs based on cylindrical PMMA optical fibers coated with an Eu^{3+} complex. A η_{opt} of 26.5% and PCE of 2.5% were reported for devices of 5 cm length and 3 mm diameter.[68] The same group reported bulk and hollow optical fibers coated or filled with a Eu^{3+} complex or rhodamine 6G. Record C values were claimed but the results were based on the light absorbed by the emitter.[100] Hydrogels based on copolymer of acrylamide, β-cyclodextrin modified with maleic anhydride, and 3-dimethyl(methacryloyloxyethyl) ammonium propane sulfonate were proposed as host matrix. The materials combine ≈90% transparency at 580 nm with flexibility and self-healing properties. Small devices were realized but no quantitative optical and electrical data were reported.[101]

5.2. Photoluminescent Emitters for LSCs

LCSs have initially employed two main classes of emitting materials, namely inorganic ions already widely used in laser glasses, and organic luminophores. The former present advantages in terms of low SA and stability while organic systems combine structural flexibility, and hence modulation of the optical properties and compatibility with various polymer host matrixes, but they often suffer from larger self-reabsorption and insufficient long-term stability under solar illumination. Recent research on organic emitters takes advantage of recent advances in the areas of FRET, solid solvation, thermally

activated delayed fluorescence (TADF), or aggregation-induced emission (AIE). On the other hand, a great deal of activity is now focused on the design of new inorganic emitters developed in the wake of the strong emergence of QDs in the past two decades.

5.2.1. Inorganic Emitters Based on Rare-Earths and Transition Metals

Inorganic emitters such as uranyl, neodymium, and holmium ions were initially investigated in the early days of LSC research but the reported performances were not really convincing.[4,13,16,84,85] Uranyl-doped PMMA was reported in 1991,[102] while more recently, an LSC based on a cerium:YAG emitter was developed as a source of intense yellow light.[103] Zero reabsorption was claimed for PMMA optical fibers doped with an europium complex.[104] Samarium-based emitters have been considered.[104,105] A PCE of 0.5% has been reported for a $2.5 \times 2.5 \times 0.1$ cm LSC transparent in the visible region with molybdenum nanoclusters as emitter.[106] Transparent LSCs were fabricated with Eu^{3+}-based bridged silsesquioxanes and Ln^{3+}, Eu^{3+}, and Tb^{3+} surface-functionalized ionosilica. Optical efficiencies of 0.29% and 0.68% (C = 0.24 and 0.54) were reported for small thin-film LSCs with terbium and europium emitters.[107,108] The photophysical properties for Zn^{2+}-induced cross-linked gold nanoclusters embedded in a rigid solid matrix have been investigated. These clusters show a ϕ_{PL} of 7.7% increasing to ≈53% in solid matrix with a blue-shifted emission spectrum due to the suppression of nonradiative relaxation and switching of emissive triplet states. An internal quantum efficiency of 34–36% was reported for thin-film LSCs of unspecified dimensions.[109]

5.2.2. Organic Emitters

Before the recent emergence of QDs emitters (see below), highly photoluminescent organic dyes have been the most widely used emitters for LSCs and the synthesis of specifically designed new dyes remains an active research field. The chemistry of organic emitters is carried out along several approaches such as the modification of the structure of existing "classical" classes of dyes, the development of new chromophore structures, the use of conjugated systems that were not initially designed as dyes, and the covalent or non-covalent combination of different chromophores in order to generate energy transfer. Other recent approaches involve the use of AIE[110] and TADF.[111] **Figure 8** shows the basic structures of the most widely employed classes of fluorescent dyes, namely rhodamines (**1**), coumarins (**2**), perylene dyes (**3**), dicyanomethylenes (**4**), and BODIPYs (**5**). Among these luminophores, the perylene dye Lumogen Red 305 (**6**) produced by BASF[112] became the "work horse" among LSCs emitters. A detailed survey of the multiple variations of these basic chemical structures is far beyond the scope of this article and the reader is referred to many existing

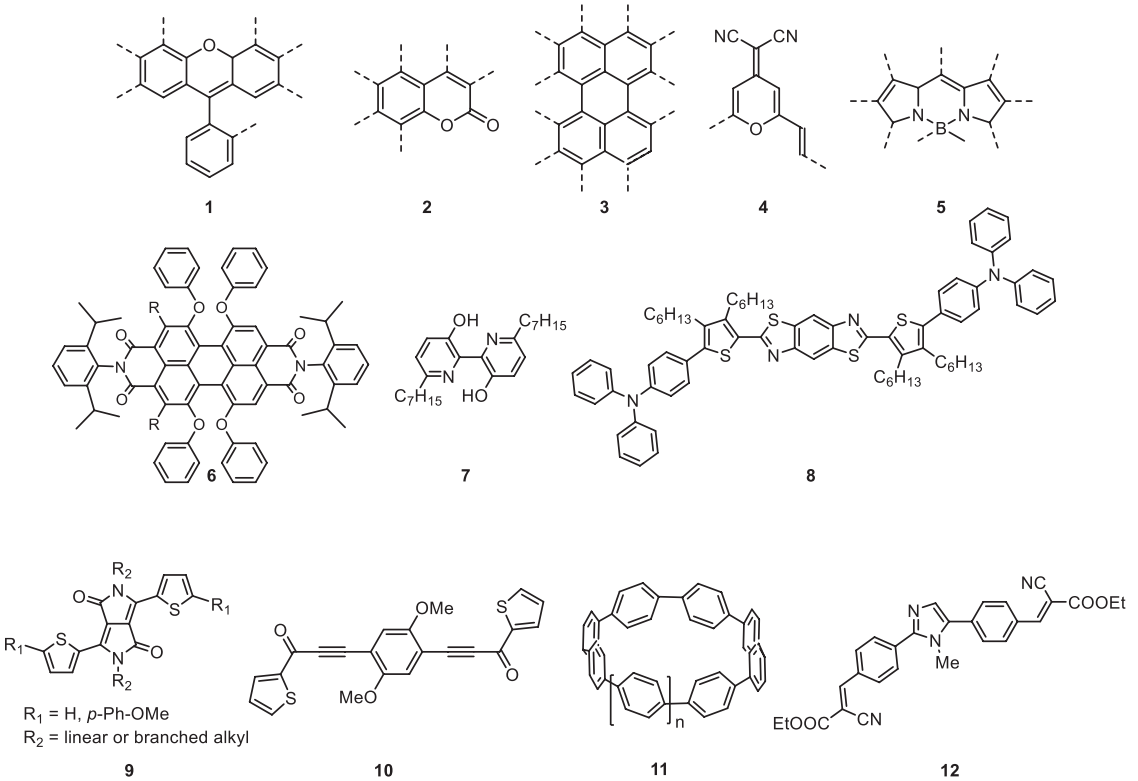

Figure 8. Generic structures of the main classes of organic emitters used in LSCs (1–5) and recent examples of organic emitters (7–12). 1: rhodamines, 2: coumarins, 3: perylenes dyes, 4: dicyanomethylenes, 5: BODIPYs, and 6: Lumogen Red 305.

specific reviews. Consequently, this part will essentially focus on the more "exotic" approaches recently developed in the field of organic emitters.

Several reports dealing with the use of emitters of biological origin have been published. Mulder et al. investigated phycobilisomes as emitters. These large water-soluble pigment–protein complexes function as light-harvesting devices in red algae and cyanobacteria and combine broad absorption in the visible spectrum and self-assembly of the tetrapyrrole chromophores in cascading FRET pathways. Evaluated in thin film and liquid LSCs, these emitters gave modest optical efficiencies of 6–12% under monochromatic light.[77] More recently, chlorophyll-based hybrid materials have been used in thin-film LSCs (7.6 × 2.6 × 0.1 cm, G = 9.7) with a maximum η_{opt} of 3.7% (C = 0.37) and a PCE of 0.10%.[113] Small liquid LSCs of 2.5 × 0.6 cm of aqueous solutions of fluorescent proteins led to an optical efficiency of 2.58%.[114] Saraidorov et al. have synthesized a bipyridyl compound locked by hydrogen bonding (**7**) as emitter combining large Stokes shift and low SA. However, the short-wavelength absorption range (300–400 nm) strongly limits the efficient absorption of the solar spectrum.[115] Besides, the widely employed Lumogen Red 305 (**6**), the chemistry of perylene dyes for LSCs remains an active field of research.[116–118] Papucci et al. synthesized green/yellow-emitting conjugated heterocyclic fluorophores (**8**) and evaluated them in 5 × 5 × 0.3 cm thin-film LSCs. Optical efficiencies of 6.4% and 7.2% corresponding to C values of 0.96 and 1.08 were reported.[119] Lucarelli et al. synthesized the first examples of diketopyrrolopyrrole fluorophores specifically designed for LSCs (**9**). A dithienyl derivative with $\phi_{PL} \approx 50\%$ evaluated in thin-film glass LSCs (5 × 5 × 0.3 cm, G = 13.3) led to an optical efficiency of 6.8% (C = 0.9).[120] Conjugated fluorophores based on bis[1-(thiophenyl)propynones] (**10**) have been employed as emitter for colorless LSCs. Evaluation in thin-film devices (5 × 5 × 0.3 cm) led to η_{opt} = 7.7%, but technical details were lacking.[121] Cycloparaphenylenes (**11**) with very large Stokes shift and low SA have been described. Optical efficiencies of 3.8% and 11% were reported for devices of unspecified characteristics based on compounds containing 8 and 10 rings with a ϕ_{PL} of 14% and 78% in a PMMA matrix.[122] Marianetti et al. synthesized imidazole fluorophores (**12**) (ϕ_{PL} = 0.15–0.25). Small thin-film LSCs (5 × 5 × 0.3 cm, G = 13.3) led to a η_{opt} of 7%, (C = 0.32).[123] In 1977, Zewail and co-workers initially proposed FRET as a possible strategy to improve solar light absorption and they reported experimental results with rhodamine 6G and coumarin.[3] Upon renaissance of LSCs, the possible use of FRET was rediscussed and investigated by several groups.[124–130] Thin-film LSCs with an emitting system based on FRET between rubrene and a dicyanomethylene dye have been investigated. A C of 8 under monochromatic irradiation was estimated from an EQE spectrum and a PCE of 6.8% was projected for tandem systems.[65] Swager and co-workers investigated energy cascades using two different conjugated polymers and Red 305 as acceptor, but only simulated LSCs results were reported.[125] Multi-BODIPY systems arranged in order to realize an energy cascade between BODIPYs of different energy levels, and, thus, extend the absorption coverage of the solar spectrum have been described.[126,127] Davis et al. reported versatile star-shaped donor-acceptor molecules based on a central BODIPY acceptor with oligofluorene donor side units in order to mitigate reabsorption by shifting the emission away from the main absorption peak. LSCs of 10 × 10 × 0.3 cm (G = 8.3) provided with four Si cells gave a PCE of 2.44% and IQE of 38.2% leading to C = 3.2 based on the absorbed light and 0.20 under white light illumination.[128] LSCs containing one to three BODIPY dyes have been investigated and a large increase of the output luminescence compared to single dye system was observed.[129] A PCE of 3.6% has been reported for a 5 × 5 × 0.5 cm LSC (G = 2.5) with a two commercial dyes as FRET emitter. The obtained C value of 0.8 was claimed as the highest ever reported (sic).[130] Some recent works have developed luminophores endowed with AIE[110] as a possible approach to limit SA.[131–137] In AIE systems, the energy cost required to form the emissive aggregated state should result in a larger Stokes shift than that of the chromophore in diluted solution. Banal et al. investigated a small thin-film LSC (1 × 1 × 0.1 cm, G = 2.5) with tetraphenylethene (TPE) (**13**) (the archetype of AIE-gen) (**Figure 9**), as emitter. Measurements with an integrating sphere gave a η_{opt} = 0.132 (C = 0.33).[131] Several extended twisted derivatives of TPE, e.g., **14**, **15** were synthesized and their photophysical properties as well as the expected performances of the resulting LSCs were reported.[131] The same group synthesized gem-dipyrene (**16**, **17**) as emitters for transparent LSCs. Evaluation of thin-film devices (2.5 × 2.5 × 0.1 cm, G = 12.5) showed that the current density of an attached silicon silver PV cell drops from 44.0 mA cm^{-2} under direct illumination to 0.80 mA cm^{-2} after coupling with the LSC, corresponding to a PCE of 0.32%.[132] In another article, the same group investigated the light-harvesting properties and SA of an emitting system involving an energy transfer between an AIE-gen **18** and a DCM dye **19**.[133] LSCs based on the AIE-gen molecule **20** (1.8 × 1.8 × 0.5 cm and 0.2 cm) (G = 0.9 and 1.8) gave a maximum η_{opt} of 4.5% corresponding to C = 0.08. It is worth noting that the fabrication of an LSC with G < 1 shows that the concentration of solar light is no longer an objective for these authors.[135]

Lyu et al. have designed an emitting material based on FRET between an AIE-gen conjugated polymer (**21**) as donor and a perylene dye (**22**) as acceptor. A 4.5 × 4.5 × 0.3 cm LSC (G = 3.75) with an optimized donor-acceptor ratio exhibited an internal optical efficiency of 20% and a η_{opt} of 5.5%, leading to C = 0.19.[137] Very recently Mateen et al. reported a first example of LSC with a TADF emitter (**23**) (Figure 9). Although limited SA was demonstrated, the performances of LSCs remain modest. Thus, a 7.5 × 7.5 × 0.3 cm (G = 6.25) showed a η_{opt} of 10.4% (C = 0.65) and a PCE of 2.2%.[138]

5.2.3. Emitters Based on QDs and Nanocrystals

Reabsorption of the luminescence and insufficient long-term stability of organic emitters remain major obstacles to the industrial development of LSCs. In this context, the perspectives of BIPV application and the strong emergence of QDs as possible emitters for LSCs have strongly contributed to the renaissance of the topic. Interest in QD emitters is motivated by a combination of several specific properties such as the possibility to modulate the absorption threshold by the control of the diameter of the dots, a high ϕ_{PL}, and high stability.[139] The applications of QDs in solar technologies have been

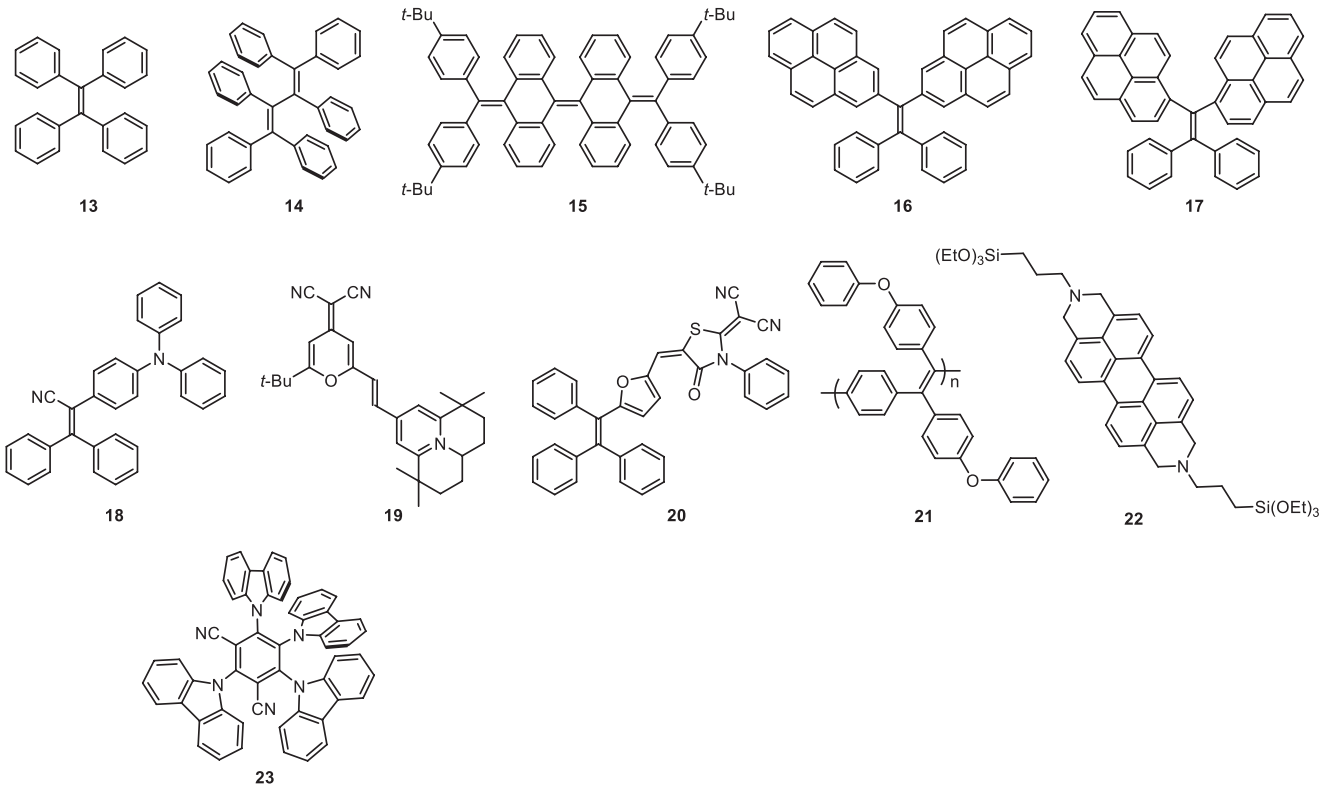

Figure 9. Chemical structures of AIE and TADF emitters.

presented in recent reviews[140–144] and this paragraph will mostly discuss recent experimental results on QDs-based LSCs. QDs were initially modelized as possible emitters for LSCs by Barnham and co-workers at the turn of the millennium.[145–147] LSCs were fabricated by spreading a suspension of CdSe/ZnS QDs in polyurethane in PMMA molders to produce 11.5 × 11.5 × 0.3 cm LSCs (G = 16.6 and 40). Although several devices gave better results than a similar device devoid of emitter, the reported C values (0.10–0.20, best value 0.29) showed that the attached PV cells always deliver less power than when directly facing the illumination source.[69] The photostability of LSCs doped with Red 305 and QDs emitters has been investigated and it was found that under constant irradiation, photo-degradation of the QDs LSCs was approximately five times slower than that of the dye-LSC. Furthermore, the QD-LSCs were reported to recover their initial absorption after a prolonged storage in the dark.[148] Bomm et al. fabricated QD-doped PMMA LSCs and reported a PCE of 2.38% for a 5 × 3 × 0.4 cm device (G = 2.35) doped with CdSe core/multishell QDs. On the other hand, stability tests revealed a minor decrease in photocurrent upon an equivalent of 3 months of outdoor illumination.[149] The results of a comparative analysis of the SA of dyes commonly used in LSCs (rhodamine 6G, Lumogen Orange, Lumogen Red), and colloidal CdTe/CdSe type-II hetero-nanocrystals (NCs) showed that reabsorption losses of type-II CdTe/CdSe NCs were negligible compared to the other luminophores investigated.[150] Erickson et al. fabricated LSCs doped with zero-reabsorption colloidal Mn^{2+}-doped ZnSe NCs as emitters (**Figure 10**). An absence of luminescence SA and an optical quantum efficiency of 37% were reported for a 2.5 × 7.5 × 0.042 cm LSC.[151]

Meinardi et al. developed "Stokes-shift-engineered" CdSe/CdS QDs with giant shells (giant QDs) to synthesize emitters devoid of SA. Increasing the number of CdS monolayers in CdSe/CdS QDs produces a progressive red shift of the emission spectrum, leading to the elimination of the overlap between absorption and emission. These QDs were then incorporated into PMMA matrixes to produce composite materials of high optical quality. The analysis of the output PL intensity as a function of the optical path (d) reveals an attenuation of ≈60% due essentially to losses associated with light-transport, a result in agreement with the early conclusions of Thomas et al.[21] A bulk LSCs 21.5 × 1.3 × 0.5 cm (G = 43) surrounded by white diffusing reflectors (DRs) gave an optical efficiency of 10.2% and C = 4.4 based on the absorbed light, and η_{opt} = 1.0% and C = 0.43 based on the incident light.[67]

Tailored CdSe/CdS NCs in poly(lauryl methacrylate) have been used in thin-film LSCs on glass substrate (48 × 65 × 0.17 mm) with an imbedded bottom micro-PV cell of 0.15 mm^2. The devices were then locked into a reflecting cavity with a highly efficient wavelength-selective top mirror. Such an environment allows a significant reduction of cone escape and scattering losses. A C value of 30.3 was claimed for blue photons. However, this result was calculated using an unusual definition of G based on the ratio of the area of an illuminated zone and of the output edge.[70] Using a rather similar experimental setup, Song et al. used a new generation of thick-shell CdS QDs with very high ϕ_{PL} > 95% and large Stokes shift in order to test the concentration limits attainable with QDs. Measurements were performed on a toluene solution of QDs placed in a cuvette inserted in a reflecting cavity covered with a selective

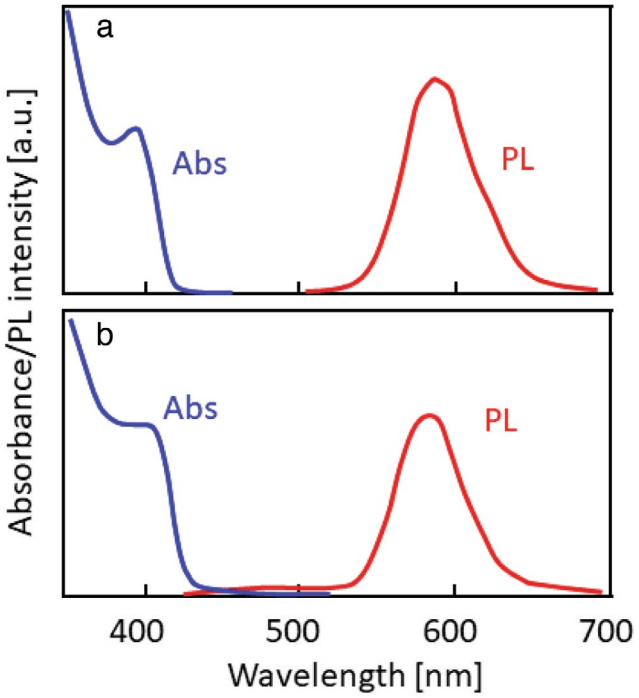

Figure 10. Absorption and PL spectra of colloidal Mn^{2+}-doped ZnSe/ZnS QDs in a) toluene and in b) an LSC device. Adapted with permission.[151] Copyright 2014, American Chemical Society.

mirror. The emitted light was collected through a bottom aperture of variable size. A C value of 60 was claimed using the integrated luminescence spectrum and the authors own definition of G based on the illumination area or output aperture.[71] Meinardi et al. used QDs of ternary I–III–VI2 semiconductors to fabricate LSCs with reduced reabsorption, extended coverage of the solar spectrum, and the absence of toxic elements. The incorporation of $CuInSe_xS_{2-x}$ QDs into photo-polymerized poly(lauryl methacrylate) leads to freestanding, colorless slabs that introduce no distortion to perceived colors and are, thus, well suited for the realization of PV windows. The reabsorption was evaluated by recording the emission spectrum after optical paths of increasing length and 30% loss was observed after a 12 cm path length. Square LSCs of 12 × 12 × 0.3 cm (G = 10) with excellent transparency in the visible spectral range were coupled to silicon PV cells. Under AM 1.5 simulated solar light, PCE values of 1.02% and 3.27% were reported for devices doped with 0.30% and 0.50% QDs, respectively.[152] Li et al. reported LSCs fabricated from core–shell giant $CdSe/Cd_{1-x}Zn_xS$ QDs, with thick $Cd_{1-x}Zn_xS$ shells in order to minimize SA. An outer silica layer isolates them from the environment allowing the preservation of a high ϕ_{PL} of 70%. Thin-film LSCs were fabricated by doctor blade deposition of a 50 µm layer of polymer/QDs on glass substrates of 1.59 mm thickness and 2.54–20.32 cm length (G = 4–32). The edge emission showed a 32% relative decrease as the length increases from 2.54 to 10.16 cm. Optical efficiencies of 30% and 17% and C values of 2.7–1.2 were reported based on the absorbed light. However, the ratios of J_{sc} values of PV cells connected at the output of the LSC or directly facing the light source gave C values of 0.65 and 0.58.[153] Giant $CdSe/Cd_xPb_{1-x}S$ core–shell QDs were used as emitters in a PMMA matrixes, resulting in a highly transparent composite with low reabsorption losses. LSCs (7 × 1.5 × 0.3 cm) with three mirrored edges (G = 23) gave an optical efficiency of 5.3% based on the absorbed light while measurements of the in/out ratio of J_{sc} values of PV cells gave an efficiency of 1.2% corresponding to C = 0.28.[154] Ultrasmall PbS QDs embedded in an acrylic matrix have been used to fabricate LSCs of 10 cm in length of unspecified geometry and other dimensions. An optical efficiency of 1.02% (claimed as a record) was reported for a G = 50 device (C = 0.50).[155] Sumner et al. have reported a detailed analysis of optical losses in polymer LSCs based on NCs of $CuInS_2/CdS$ as emitters. LSCs of 7.5 × 7.5 × 0.10 cm of NC-containing poly(lauryl methacrylate-*co*-ethylene glycol) layer sandwiched between two 0.90 mm thick glass sheets led to an overall device thickness of 2.8 mm (G = 6.7). The best device gave an optical efficiency of 5.7% (C = 0.38). It was concluded that waveguide losses grow in proportion to NC loading and that scattering losses from NC aggregates become limiting in larger devices.[156] Tummeltshammer et al. synthesized an original hybrid system in which a high ϕ_{PL} organic dye is linked to a QD with high absorption profile in order to improve the limited PL efficiency of the QD by FRET process. Comparative evaluations were performed in water solutions contained in a 2 × 2 × 0.3 cm cuvette (G = 7.3). Under monochromatic illumination, internal optical efficiencies of 15.9%, 14%, and 19.8% were reported for the QD, the dye, and the FRET system, respectively, thus confirming the improvement due to FRET. Under simulated solar light, measurement of P_{in}/P_{out} with silicon PV cell gives a PCE of 2.87% and C = 0.22.[79] Wu et al. fabricated a tandem system consisting of two thin-films LSCs based on two types of QD emitters. The top LSC involves highly emissive Mn^{2+}-doped Cd_xZn_{1-x} S-based QDs with an absorption onset at ≈440 nm and ϕ_{PL} = 72%. Due to efficient excitation transfer from the semiconductor host to the emissive Mn^{2+} ions, emission occurs in a reabsorption-free intragap region. The bottom device contained narrow band gap $CuInSe_2$ (CISe)-based QDs that exhibit strong absorptance across the solar spectrum and ϕ_{PL} = 65–75%. Under solar illumination 10 and 15 cm square LSCs gave C values of 1.44 and 1.77. The tandem system shows an internal optical efficiency of 6.4% (based on the absorbed light) and a PCE of 3.1% under sunlight illumination.[157] In view of the potential problems posed by the toxicity of metals such as cadmium or lead, Meinardi et al. have proposed to use earth-abundant silicon QDs as nontoxic emitters. Inserted in PLMA matrix, the emitter shows a ϕ_{PL} of 0.46 and an emission maximum at 800 nm with a good optical transparency in the visible spectral range. The small overlap of the emission and absorption spectra suggested small reabsorption losses, as confirmed by experiment. Under AM 1.5 simulated solar light, a 12 × 12 × 0.26 cm device (G = 11.5) with peripheral silicon PV gave an optical efficiency of 2.85%, corresponding to C = 0.33.[158] Attempts to improve the efficiency of LSCs based on $CuInS_2/ZnS$ by introduction of SiO_2 particles in order to induce a scattering effect have been reported. A PCE of 4.20% was obtained with a 2 × 2 × 0.8 cm device (G = 2.5) and a 60% improvement was claimed versus a device devoid of SiO_2 particles.[159] In contrast, other authors have tried to limit scattering in LSCs based on silicon QDs in PMMA. Methyl 10-undecenoate-functionalized silicon QDs have been reported

to present a low level of agglomeration in PMMA, thus leading to reduced scattering and improved light-guiding properties.[160] Liu et al. reported a tandem device with a thin film of carbon dots (CDs) as top LSC and a CdSe/CdS QDs as bottom device. The resulting 10 × 10 × 0.20 cm semitransparent tandem exhibits an optical efficiency of 1.4% under one sun illumination. The top CDs LSC was reported to significantly improves the photo-stability of the bottom LSC under UV illumination.[161] LSCs based on a film of CdSe/CdS QDs dispersed in toluene and mixed with polystyrene sandwiched between two glass plates have been described. The analysis of the PL emission as a function of the distance between an illuminated spot and the output edge revealed a ≈80% attenuation after 10 cm. Comparison with a simple plate LCS 10 × 10 × 0.4 cm ($G = 6.25$) shows that the sandwich structure improves η_{opt} from 1.66% to 2.02% with a maximum of 2.95% ($C = 0.16$), while a PCE of 2.25% was obtained with a silicon cell.[162] Mazzaro et al. reported an original approach involving the coupling of an organic dye to silicon NCs in order to sensitize their luminescence. Energy transfer was investigated by optical and PV experiments. A η_{opt} of 4.25% was determined with PV cells and 38.8% based on the absorbed light. With a $G = 2.6$, these results correspond to $C = 0.11$ or 1.65 based on absorbed light.[163] Thin-film LSCs of Si QDs in PMMA deposited on glass by doctor blade have been investigated. Quick solidification of PMMA leads to low light-scattering films with an order of magnitude higher QD weight fraction than previously reported non-scattering bulk-polymerized Si QD/PMMA nanocomposites.[164] 3D macroporous photonic crystals have been proposed for the fabrication of efficient photon reflectors for QD-coated LSCs. Characterization of a 2.8 × 1.5 × 0.1 cm device with an integrating sphere showed that adapting the reflection band to the emission profile of the QD emitter improves the light-trapping efficiency from 73.3% to 95.1%. However, the reflectivity of the stop band filter poses the problem of light-guiding by TIR over long distances, and, hence, in large-area LSCs.[165] LCSs have been fabricated by laminating an acrylate layer containing 0.4 wt% of $CuInS_2$/ZnS QDs between two glass plates. Comparison of different types of glasses showed that those with low iron content gave much higher efficiencies of 4.4% versus 1.0%. A 100 cm^2 device of unspecified thickness gave a PCE of 2.18% under simulated solar light increasing to 2.94% with a back reflector. A record optical efficiency of 8.1% with monochromatic LEDs as an excitation source was claimed for a 10 × 10 cm device but surprisingly the back reflector did not change this value.[166] Anand et al. reported semitransparent LSCs with 60% absorptance in the 400–750 nm spectral range. Stoichiometric $CuInS_2$ emitters of ≈1.5 nm were reported as the best trade-off between broadband absorption and reabsorption. Under outdoor perpendicular illumination, a 30 × 30 cm = 900 cm^2 ($G = 10.7$) device delivers a PCE of 6.8%, which is the highest reported to date for an LSC of this size. The device shows an optical efficiency of 7.40% (29.2%, based on absorbed light) and $C = 0.75$ (3.12 based on absorbed light).[167]

The toxicity of classical QDs containing metals such as Cd or Pb has triggered the search for alternative nanomaterials as emitters. Besides the already discussed silicon QDs,[158,160,163,164] several groups have investigated CDs as possible nontoxic emitters.[161,168–176] Zhou et al. prepared CDs modified by a treatment with oleylamine in order to reduce absorption in long wavelengths, and thus, SA. These CDs were incorporated in poly(lauryl methacrylate) matrix to produce bulk LSCs. An optical efficiency of 1.20% was reported for a 1.5 × 2 × 0.2 cm with three mirrored edges ($G = 10$, $C = 0.12$), decreasing to 0.40% for $G = 38$ ($C = 0.15$).[169] LSCs with a high loading of CDs have been fabricated by in situ cross-linking of organosilane-functionalized CDs. Although the emitter still presents good emission efficiency in the solid state, the PL spectra recorded at various concentrations reveal significant reabsorption. LSCs of 3.0 × 3.0 × 0.3 cm ($G = 2.5$) were fabricated and an optical efficiency of 12% was obtained under monochromatic irradiation at 354 nm.[170] Thin-film LSCs were fabricated by spin-casting PMMA films from solutions containing various concentrations of N-doped CDs on glass slides of 2.5 × 1.6 × 0.1 cm ($G = 4.9$). The PL spectrum reveals a strong dependence on the excitation wavelength, suggesting a polydisperse emitter. The optical efficiency was found to increase with film thickness from 2.60% to 4.75% corresponding to C increasing from 0.12 to 0.23. It is noteworthy that a reference undoped device already gives a η_{opt} of 1.9% and $C = 0.09$.[171] Devices based on thin films of CDs-doped polyvinylpyrrolidone on glass gave rather similar results ($C = 0.20$ at $G = 4.1$). Surprisingly the reported PCE (4.97%) was practically equal to the optical efficiency (5.02%).[172] On the other hand, the same CDs imbedded in a PMMA host matrix 2 × 2 × 0.2 cm ($G = 2.5$) gave a maximum η_{opt} of 12.23% ($C = 0.31$) and PCE = 2.63%. A similar device devoid of emitter already gives η_{opt} and PCE of 7.58% and 1.48%, respectively.[173] CDs have been combined with nanoparticles of a TPE rhodanine AIE-gen to fabricate LSCs of 2.5, 4.5, and 6.5 cm length and 2.0 cm width. The PCE of the CD-doped LSCs decreases with their length from 1.76% to 1.51%, that of the AIE-NP device from 2.30% to 2.04% and that of the tandem device from 4.06% to 3.55%. In contrast, doubling the thickness of the 2.5 cm long CD-doped LSC from 1 to 2 mm (thus reducing G from 3.6 to 1.8) increases PCE from 1.76% to 2.30%.[174] Mateen et al. reported tandem LSCs combining organic dye-doped and CD-doped devices. The CD top slab was a thin-film device of 5 × 5 × 0.3 cm and the bottom device was a bulk PMMA LSC doped with two organic dyes. The dye-doped LSC gave η_{opt} and PCE of 13.4% and 2.72%, respectively, ($C = 2.2$ at $G = 16.6$), while the single CD-doped plate gave a η_{opt} of 5.62%, a PCE of 1.03%, and $C = 0.87$. A PCE of 3.20% was reported for the tandem device equipped with a back reflector.[175] Organosilane-functionalized CDs cross-linked in a siloxane matrix have been used to fabricate thin-film LSCs on glass substrates. At a 10% loading, the CDs present a high ϕ_{PL} of 94%. An LSC of 3 × 3 × 0.3 cm ($G = 3.33$) shows a η_{opt} of 3.9% ($C = 0.13$).[176]

5.2.4. Perovskite Emitters

The use of perovskite emitters in LSCs was initiated by Mirershadi et al. who reported an improvement of up to 45% of the efficiency of a silicon PV cell irradiated with a mercury lamp when covered with a wave-shifter containing $CH_3NH_3PbBr_3$ in polyvinyl alcohol.[177] Meinardi et al. reported manganese-doped $CsPbCl_3$ NCs as reabsorption-free emitters for large-area LSCs. Light propagation measurements revealed very weak

reabsorption and it was concluded that the system is close to an ideal behavior. A 25 × 20 × 0.5 cm device (G = 50) with silicon PV cells gave a PCE of 0.5% with C = 0.25.[178] Zhao et al. synthesized mixed-halide perovskite $CsPb(Br_xI_{1-x})_3$ QDs with absorption ranging from 300 to 650 nm, a small overlap of absorption and emission spectra and a ϕ_{PL} > 60%. Semitransparent LSCs of 9.0 × 1.3 × 0.2 cm and G = 45 exhibit an external optical efficiency of 2.0% (C = 0.9).[179] Shortly after the same group reported a tandem system with a CD top slab and perovskite bottom slab with η_{opt} of 3.0%.[180] Luo et al. introduced the concept of quantum-cutting LSCs using Yb^{3+}-doped perovskite NCs. These emitters combine a ϕ_{PL} approaching 200% and virtually no self-reabsorption of PL photons. A 25 cm^2 LSC fabricated from Yb^3-doped $CsPbCl_3$ showed an internal conversion efficiency of 118%.[181] Tong et al. synthesized potential LSC emitters based on formamidinium lead bromide ($FAPbBr_3$) NCs via solvent-induced reprecipitation using dicarboxylic acids as ligands. As-synthesized decanedioic acid (DA)-capped $FAPbBr_3$ NCs exhibit a high ϕ_{PL} of 90%. A viscous suspension of NCs mixed with toluene and polystyrene was deposited on PMMA by doctor blade and the emissive properties of small prototypes were characterized.[182] Nikolaidou et al. used ($CH_3NH_3PbI_{3-x}Cl_x$) as emitter in thin-film devices on 1.5 × 1.5 × 0.1 cm ITO substrates (G = 1.5) and reported a η_{opt} up to 30% (C = 0.45) under solar illumination.[183] More recently, the same group reported a η_{opt} of 34.7% for a perovskite LSC of unspecified dimensions.[184] $CH_3NH_3PbBr_3$ embedded in a PMMA was used to fabricate bulk LSCs of 5 × 3 × 0.5 cm in a mirror surrounded configuration (G = 10). Under AM 1.5 simulated solar light, the attached PV cells present a PCE of 9.20% in the absence of LSC and 5.44% at the LSC output, suggesting a C value of ≈0.60, while a pure PMMA device gave PCE of 3.24%, underlining once again the problems posed by very small LSCs.[185] Wei et al. synthesized perovskite nanoplatelets with a tunable number of layers within each platelet. Ultrafast, nonradiative exciton routing produces at the same time a high ϕ_{PL} and a large Stokes shift. Thin-film LSCs 10 × 10 × 0.2 cm (G = 12.5) gave internal optical quantum efficiency of 26%, an internal concentration factor of 3.3, C = 0.18, and η_{opt} = 0.87% in outdoor conditions.[186]

6. Technology of LCSs

As widely demonstrated, the efficiency of LSCs is essentially determined by the characteristics of the emitter and to a lesser extent, to those of the host matrix. However, the technical implementation of these two main components exerts a major influence on the final performances of the system. In this part, the various technological aspects of luminescent solar collectors will be briefly reviewed.

6.1. Wavelength Shifters

The conversion of solar light by a layer of luminescent material covering PV cells was initially proposed in 1979 by several authors. A fraction of the high energy incident light that would otherwise result in thermalized charge-carriers is converted into photons of longer wavelengths more efficiently converted by PV cells. Improvements of PCE of 0.50–2.0% were reported for plastic encapsulation layers doped with fluorescent dyes.[187–189] During the past decade, encapsulation by luminescent materials has been developed by several groups who combined different types of luminophores to various PV cells (silicon, GaAs, CdTe, CIGS, DSSC, and organic solar cells). This idea has been considered by theory and simulation in the case of QD emitters[190,191] and discussed in a review published in 2009.[192] A related concept involves the combination of wavelength shifters with micro-structuration of the host matrix. Thus, an 11% increase of the efficiency of PV cells placed at the bottom of funnel-shaped optical systems doped with rare earths has been reported.[193]

6.2. Bottom Cell LCSs

In bottom cells or "front-facing" LSCs, the PV cells are inserted at the bottom of a luminescent host matrix.[26,36] Such systems can be viewed as intermediate between wavelength shifters and classical edge-cell LSCs. In fact, the difference lies essentially in the volume and area of the host material. In 1983, Lifante et al. reported an improvement of efficiency of up to 30% for PV cells immersed in a fluorescent liquid medium (**Figure 11**).[26] More recently, bottom cell LSCs have been revisited by several groups.[70,71,194–196]

Corrado et al. reported C values of ≈2 for PV cells imbedded in PMMA doped with lumogen 305 and fabricated large-scale devices tested in outdoor conditions.[194] Zhang et al. fabricated a 7.8 × 7.8 × 0.7 cm bottom cell device doped with organic dyes with a PCE of 5.08% and C = 1.38.[196] While this value was claimed as a record for a doped PMMA LSC, it is markedly inferior to many previous results.[13,18,22,27,74]

6.3. Thin-Film LSCs

In thin-film LSCs, the luminophore is confined in a thin layer deposited on the top (or bottom) surface of a fully transparent matrix. Compared to bulk LSCs, this concept presents the potential advantage of simplicity of fabrication and large possibilities of combinations of emitters and waveguides. Since the emitted light is supposed to travel within a fully transparent medium, the absence of reabsorption losses and hence a much higher efficiency can be expected compared to bulk LSCs. However, the presence of the heavily doped layer on one face of the LSC can have deleterious effects on the light-guiding properties

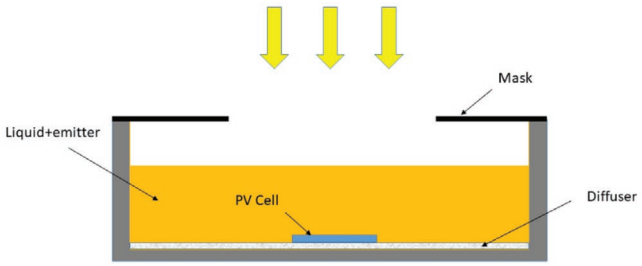

Figure 11. Bottom cell liquid LSC. Adapted with permission.[26] Copyright 1983, The Optical Society of America.

since instead of TIR, each reflection on the internal side of the coated surface may lead to isotropic reflection and scattering, and hence dramatically increase the photon escape through the opposite loss cone. In order to limit this problem, the refractive index of the thin-film material must be significantly inferior to that of the waveguide as in optical fibers.[32] However, this prerequisite is rarely taken into consideration. Already in 1970, Keil experimented a system in which a doped polymer plate was glued on a fully transparent one.[8] This concept was then extended by Friedman in early work on LSCs.[24] In 1988, Reisfeld et al. described a 10 × 10 cm LSC (G = 8.3) fabricated by casting a 50 µm film of PMMA doped with a fluorescent dye at the surface of a PMMA matrix and reported C values of 1.70 and 2.98 and efficiencies of 20.4% and 35.7% with silicon and GaAs cells, respectively.[31] It was noticed that in small devices, the dominant component of the luminescence comes to the edges directly from the thin film without undergoing multiple internal reflections.[31] Some years later, the same group reported a η_{opt} of 18.8% measured indoor on a cloudy day for a PMMA LSC 5 × 5 × 0.3 cm (G = 4.2) coated on both sides with a sol–gel solution of a perylene dye.[64] More recently, Dienel et al. reported LSCs made of microscope slides coated with PMMA containing Red 305 and reported a C of 1.30.[57] Maggioni et al. fabricated thin-film LSCs by co-evaporation under vacuum of parylene C dimer and lumogen 305 on glass or PMMA waveguides. A 5 × 5 cm LSC (G = 2.5) gave an optical efficiency of ≈5% with a silicon cell raising to 21% with a GaAS cell and a diffusing back reflector but C remained inferior to unity.[94] The effect of the thickness of the thin film on efficiency has been investigated.[197] Thin-film and bulk LSC doped with the same perylene dye have been compared on devices of 2.5 × 2.5 × 0.1 cm doped with various dye concentrations and it was concluded that bulk LSCs lead to better results than thin films.[198] In recent years, thin-films LSCs have been investigated by many groups,[107,119,131,153,157,161,162,183,184] but until now, only one example of thin-film LSC of more than 100 cm^2 area giving $C > 1$ has been reported.[157]

6.4. Geometry of LSCs

The geometric gain G of a LSC depends on the three dimensions of the system and also on its geometry. For example, for a square LSC of a given input surface, covering three sides with mirrors increases G by a factor of 4, thus allowing an increase of C without increasing the input area. The effects of G and geometry have been investigated by several groups and various shapes such as triangle, square, pentagon, hexagon, and half circle of both solid and liquid systems have been investigated. Valeur and co-workers compared triangle, square, rectangle, and half-disk liquid LSCs of 20–25 cm^2 with G of 5–40 and reported C values of 0.40–0.80, increasing to 0.80–1.30 with back reflectors. They found no significant difference among the different geometries and obtained the highest C of 1.21 with a rectangle of G = 40.[25] Roncali and Garnier fabricated LCSs of 50–400 cm^2 based on PMMA doped with two different organic dyes. Devices of triangular, square, and pentagonal geometries with all sides (except the output) covered with white diffusing mirrors were analyzed. Under monochromatic irradiation, a small effect of geometry was observed for 100 cm^2 devices with C increasing from 12 for triangles (G = 33) to C = 14 for pentagons (G = 65), while for 400 cm^2 LSCs, similar results were obtained with square and pentagon (C = 21.2 and 22, respectively, for G = 100 and 130). Based on the fact that C reaches a maximum for a certain value of G, it was concluded that for large input areas, an open square with the full perimeter covered with PV cells was the optimal solution.[27] Other works based on Monte-Carlo simulations concluded that efficiency is relatively independent of the geometry.[28,199] Sidrach de Cardona et al. investigated the variation of the output light intensity on triangles of 0.25 m^2 and found a maximum in the middle of the output edge. Based on simulation, they concluded that hexagonal devices were superior to squares.[63] Vishwanathan et al. compared planar and cylindrically bent LSCs and reported that bent systems present higher surface losses than planar devices but are less sensitive to the direction of the incident light.[200]

6.5. Cylinders and Optical Fibers

LSCs of cylindrical shape have been envisioned recently. A theoretical comparison of planar and cylindrical LSCs led to the conclusion that when PL emission occurs close to the surface, the optical concentration of a cylindrical LSC can be 1.0–1.9 times higher than that of a square planar system of equivalent input area and volume and that aligned adjacent cylindrical LSCs reflects less incident light than a planar LSC for any angle of incidence.[201] The practical implementation of cylindrical LSCs has essentially resorted to optical fibers. Luminescent fibers have been considered for lighting application but the luminous efficiency remains inferior to that incandescent light bulbs.[202] Inman et al. fabricated PMMA bulk and hollow cylindrical devices of centimeter-scale doped with PbS QDs. Planar devices of 2.5 × 2.5 cm (G = 2.3) gave η_{opt} = 4% and C = 0.10. Upscaling to 30 × 30 cm (G = 19) reduced η_{opt} to 1% while C increases to 0.19. These devices were compared to solid and hollow cylindrical devices and it was concluded that the latter absorb more incident radiation, present lower SA, and are more efficient than solid cylindrical and planar geometries of similar G values.[203] Correia et al. reported LSCs based on commercial PMMA-based optical fibers coated with an Eu^{3+}-doped organic–inorganic hybrid layer. They reported an optical conversion efficiency of 20.7% and an electrical efficiency of 2.5% based on the light absorbed in the 300–380 nm region.[68] The same group investigated long hollow optical fibers coated or filled with europium complex or rhodamine 6G. An optical efficiency of 72.4% and C = 12.2 were calculated on the basis of the absorbed light and claimed as a record. However, these values decreased to 2.3% and C = 0.4 under solar illumination.[100] Parola et al. fabricated fluorescent PMMA optical fibers double-doped by organic dyes and an europium complex by a bulk polymerization and fiber drawing. Measurement of the output power generated by a 6 cm fiber under AM 1.5 simulated solar light and with a back reflecting mirror gave a value of 31 mW cm^{-2} corresponding to $C \approx 0.30$ and a conversion efficiency of 0.41% in the best case but the output power intensity decreased to 13 mW cm^{-2} for a 6 m long fiber.[204] Recently, it was reported that the insertion

of an array of optical fibers between an LSC and a diffusing white reflector led to a significant increase of efficiency of a $10 \times 3.5 \times 0.3$ cm LSC leading to the best PCE of 0.88%.[205]

6.6. Improving Light-Trapping and Waveguide Properties

Several technological improvements involving the modification of the configuration of the LSCS have been proposed and experimentally investigated. Already in 1979, Goetzberger and Schirmer proposed to adapt a taper of higher refractive index at the output edge of LSCs in order to increase light concentration.[206] This idea was recently rediscussed.[207] Debije and co-workers have proposed patterning the dye-containing film of thin-film LSCs as a possible approach to reduce SA.[208,209] Complex modifications of the surface of LSCs have been proposed to limit reabsorption by resonance shifting,[207,210] as well as other types of surface reshaping including convex lenslet, staircase, addition of a parabolic element, or wedge shape.[207,211–213] Various approaches have been proposed to increase the trapping efficiency including back reflectors, photonic band filters, and control of chromophore orientation. It has been shown that a reflector placed behind the LSC can significantly improve the efficiency and that DRs gave better results than specular mirrors.[22,23,26,27,29,30,55] A detailed investigation of the effects of the relative size and orientation of DR was carried out by Lifante et al. who reported a 80% increase of efficiency for a 100 cm^2 LSC with a DR that largely exceeds the size of the LSC.[214] DR was recently reconsidered both experimentally and theoretically confirming earlier conclusions.[38,62,128,215–219] With a specular reflector, the light not absorbed during the first crossing of the LSC is reflected in the same direction and photons of wavelengths longer or shorter than the absorption of the emitter have little probability to be absorbed or scattered during the back trip. With a DR, unabsorbed photons are isotropically reflected. In the neighborhood of the output edge(s), the reflected light that contains both luminescence photons lost by the LSC and the unabsorbed light, including the "more efficient" long wavelength photons can directly reach the PV cell (**Figure 12**). A DR, thus, generates a "recovery zone" the extent of which depends on the thickness of the LSC.[30,31] Since the extent of this zone is independent of the size of the LSC, its relative contribution is much larger for small devices, and thus represents a major cause of the overestimation of the efficiency of very small LSCs. In fact, contrary to the expected improvement of efficiency, the direct application of a white diffusing layer on the external bottom side of an LSC produces a dramatic deterioration of the light-guiding properties since instead of TIR, every photon striking the back internal surface is isotropically reflected.

Thus, after a few reflections on the internal bottom surface, the largest fraction of the emitted light leaves the LSC through the top loss cones. Note that this phenomenon that occurs in thin-film LSCs when the refractive index of the thin film is too low constitutes a major limitation for light-transport and efficiency in these systems, except for small devices where

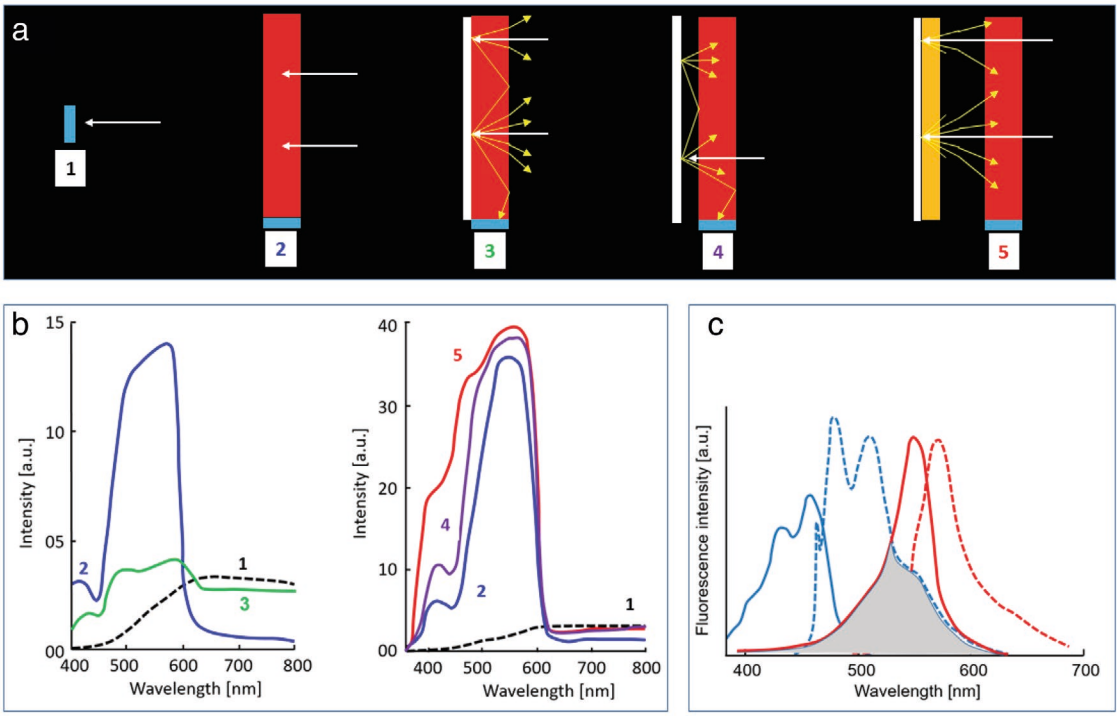

Figure 12. a) Effects of back reflectors. 1: PV cell alone; 2: PV cell coupled to an LSC (triangle 43 cm^2); 3: same as 2 with a white diffusing layer applied on the backside of the LSC, this allows the capture of long wavelength photons but destroys light-guiding; 4: LSC (square 400 cm^2) with independent DR; 5: LSC with active reflector. b) Spectral responses of the PV cell for cases 1–5. c) Absorption and emission spectra of the dyes of the active reflector (blue) and LSC (red). The gray zone corresponds to the recoverable light from the front emission of the active reflector. Adapted with permission.[30] Copyright 1984, Elsevier.

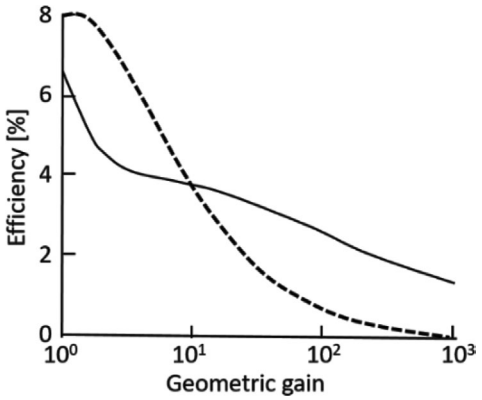

Figure 13. Calculated electrical efficiency versus geometric gain for an infinite ribbon LSC with PV cells on both sides. The dotted line represents the performance of a scattering plate of identical geometry. Adapted with permission.[18] Copyright 1981, The Optical Society of America.

scattering effects can be predominant.[18,59,159,171,173] In fact, as already underlined by Zewail in 1981, for $G < 10$, a purely scattering plate can outperform a doped LSC (**Figure 13**),[18] a conclusion supported by several recent experimental results on non-doped matrixes.[69,171,173] This deleterious effect can be turned into advantage by the concept of active DR. A white diffusing layer is applied to the back side of a polymer slab containing a luminophore that absorbs at shorter wavelengths than the LSC emitter but emits in its absorption range. Short wavelength photons cross the LSC, excite the DR luminophore, are reemitted at longer wavelengths through the top surface of the DR and are absorbed by the LSC during the back trip. An active DR, thus, improves the capture of long wavelength photons and extends the spectral response of the LSC in the short-wavelength region (Figure 12). These combined effects produce a significant increases of efficiency under white light illumination; thus, C values of 22 and 9 were obtained under, respectively, monochromatic and white light illumination of a 400 cm^2 square LSC ($G = 130$).[30] To the best of our knowledge, these C values remain the highest reported so far for LSCs.

6.7. Recent Technological Advances

The new wave of LSC research has generated several technical innovations for loss mitigation leading to a what has been qualified as "second-generation LSCs."[220] Band stop filters made of high dielectric constant materials have been suggested as a possible solution to limit photon escape through the loss cone[39,41] and investigated by several groups.[70,71,220–226] A commercial polymer opal photonic filter has been reported to increase the optical efficiency of a 50 cm^2 LSC from 2.6% to 3.1%.[217,221] Debije and co-workers reported that a cholesteric mirror separated by an air gap from the top of a LSC reduces the surface losses and leads to a 12% increase of η_{opt}.[222,223] Distributed Bragg reflectors fabricated by spin-casting alternating layers of SiO_2 and SnO_2 nanoparticle suspensions onto glass substrates have been fabricated in order to define design rules for light management in LSCs.[225] More recently, it was reported that Bragg stacks with photonic band-gap tuned to the long wavelength side of the dye emission spectrum lead to an increase of η_{opt} from 9.4% to 10.3% ($C = 0.75$–0.82) of a $2.4 \times 2.4 \times 0.3$ cm LSC ($G = 8$).[226]

6.8. Orientation of the Luminophore

Another approach to limit the loss of photons through the escape cone is based on the control of the direction of the PL emission by orientation of the chromophore.[227–233] While this idea has been essentially developed in recent work, it was already discussed by Zewail et al. in 1979.[15] Debije and co-workers investigated the alignment of three organic dyes using liquid crystals host material. Measurements of the output luminescence from an edge parallel to the alignment direction of 3×3 and 5×5 cm thin-film LSCs showed a 25–30% increase of intensity over isotropic system. This effect was reduced when part of the perimeter of the LSC was covered with mirrors.[227] MacQueen et al. reported that the homeotropic alignment of perylene dyes in nematic liquid crystals produces a decrease of surface losses.[228] Mulder et al. investigated the effects of vertical and horizontal chromophore orientation and reported an increase from 66% to 81% of the trapping efficiency of thin-film LSC by vertical alignment of coumarin molecules with polymerized liquid crystal host (**Figure 14**).[230] A combination of chromophores with positive and negative dichroism has been proposed in view of developing advanced light management in LSC windows.[231]

A major problem posed by the vertical orientation of dipolar rod-shaped chromophores is that this alignment that reduces surface losses is detrimental to the absorption of the incident light. In order to address this problem, Zhang et al. recently reported an original approach based on the combination of a sphere-shaped energy donor and a rod-shaped emitter perpendicularly aligned by means of a polymerized liquid crystal matrix. An increase of trapping efficiency from 72% to 79.3% was reported together with reduced SA.[233] Until now, chromophore alignment has been essentially achieved using liquid crystal matrixes. It is rather surprising that poling under electric field, widely employed to produce non-centrosymmetric materials for second-order nonlinear optics, has not been considered so far.[234]

7. Applications of LSCs

Although PV conversion remains the main application, the spectrally managed luminous energy produced by LSCs can be also used in other applications either as direct light source or after conversion into other forms of energy. Thermal energy conversion was proposed in 1979 by Goetzberger. High temperatures were reached in a pipe-collecting system placed at the output of LSCs (555 °C in AM 1.5 conditions and 250 °C under diffuse light) but this idea was not further developed.[14,235] LCSs have been proposed for the design of position-sensitive devices[236] to limit the temperature of PV cells in a space environment,[237] or to convert the light of LEDs used for pumping organic semiconductor lasers.[238]

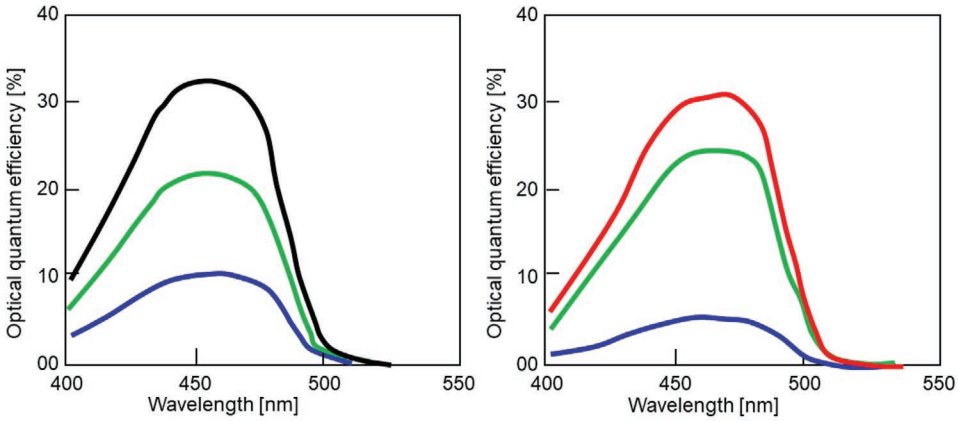

Figure 14. Optical efficiency of the facial emission (blue), edge emission (green), and total emission (red) of left) isotropic and right) vertically aligned LSCs doped with coumarin 6. Adapted with permission.[230] Copyright 2010, The Optical Society of America.

Fiber-coupled LSCs have been proposed as broadband light source for medical diagnosis, light detection,[239] or for lighting applications.[38,240,241]

While the term "greenhouse solar collector" was used in a metaphorical sense by Weber and Lambe in their founding article of 1976,[1] the use of luminescent materials in real greenhouses has received some attention. Selective light-filtering plastic films for plant greenhouses have been investigated.[242–245] Whereas an increase of the production of strawberries or roses has been claimed,[243] other studies reported no significant effect.[242] Recently, this idea was reinvestigated and a film of PMMA doped with a fluorescent coumarin dye was developed in order to convert the absorbed light into the absorption range of chlorophyll.[244] A major problem is that, except for a simple filtering effect, the plants receive only the fraction of the spectrally tuned emitted light of the loss cone, a major part being guided to the edges of the film. Thus in contrary, to LCSs, such an application requires an optimization of optical losses through the internal side of the film using, for example, a matrix with a gradient of refractive index or by inclusion of scattering centers. An interesting utilization of LSCs recently reported consists in the immersion of the bottom part of the specifically designed LCSs in the liquid-growing medium of *Arthrospira platensis* algae (**Figure 15**). This system leads to 26% and 44% improvement in the production of biomass and phycocyanin, respectively.[246,247] The use of LSCs to transfer light from the highly illuminated above canopy zone to low canopy plants has also been suggested.[240]

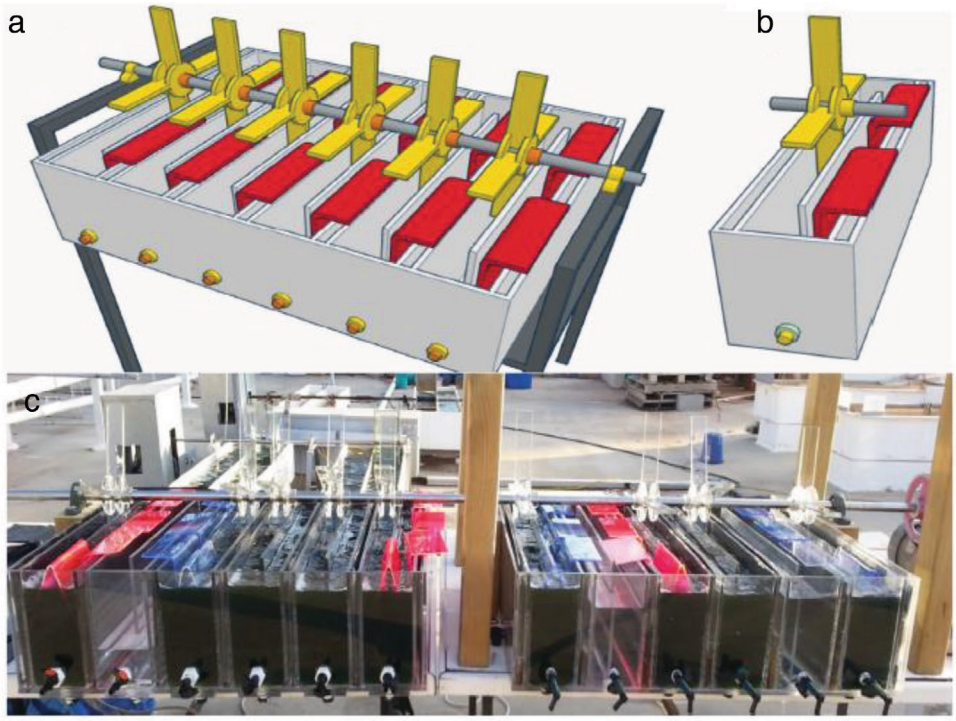

Figure 15. LSC-assisted growth of *Arthrospira platensis* algae. Reproduced with permission.[246] Copyright 2020, Elsevier.

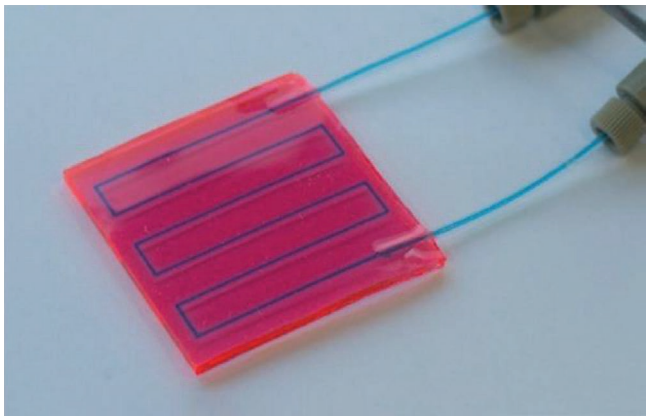

Figure 16. Photograph of a continuous flow LSC-photomicroreactor. Reproduced with permission.[251] Copyright 2017, The Royal Society of Chemistry.

It has been shown that the chemical potential of the edge fluorescent flux of an LSC is identical to that of the excited state of the emitting dye.[248] Some recent publications have reported the use of the light emitted by LSCs to produce photochemical reactions.[249–254] Debije, Noël and co-workers have developed PDMS LCSs doped with fluorescent dyes to convert sunlight into a narrow spectral band and transport that energy to embedded microchannels to produce photochemical reactions (**Figure 16**).

The validity of the concept was first demonstrated for the photooxidation of diphenylanthracene and then extended to various photochemical reactions such as photo-oxidations, photocatalytic trifluoromethylation chemistry, metallaphotoredox transformations, or preparation of medicinally relevant molecules.[249,250] The system was then modelized from both optical and fluid dynamics viewpoints and scaled-up to a device involving 32 parallel microchannels embedded in an LSC converter.[251–253] Liu et al. have used a LCS doped with giant QDs to irradiate a photoelectrochemical cell for hydrogen production.[254] Although a significant improvement of stability was reported, the photo-current drops by one order of magnitude with a LSC as irradiation source.

The renaissance of LSCs is associated with the emergence of building integrated photovoltaics (BIVP). A general context marked by environmental concerns and energy savings has triggered the exploration of many niches of energy resources potentially available in urban environment.[6,7,255–263] Debije and co-workers have fabricated large-scale LSCs to serve as noise barrier in urban environment and investigated the effect of light orientation and street art on the performances.[260,261] Luminescent tiles based on LSCs with bottom solar cells have been developed for roof application.[262,263] Perhaps the most promising field of application of LSCs in urban environment lies in the considerable collecting surface for solar light offered by the windows of modern buildings.[6,7,255–259] However, the use of LSCs for this application poses problems related to technical and economic aspects and social acceptability. Efficiency under diffuse light and limited angular dependence on incident light are specific advantages of LSCs for BIPV[5–7,257,265] in addition to their multiple possibilities of color and shape that also open large possibilities for artistic creation.[264,266–269] For example, Kerrouche et al. have analyzed a large number of LSCs of various shapes and colors and presented a model of artistic stained-glass window with an optical peak power of 5 W under 1000 W m^{-2} illumination.[266] The design of LSCs for solar window application cannot exclusively focus on performances but requires the definition of appropriate balance between efficiency, optical transparency, and social acceptability.[6,7,270–274] This problem is far from trivial since until now, large-scale LSCs are poorly efficient and a constraint of transparency can impose a further limitation to the efficiency. Wiegman et al. investigated the optical properties of an LSC based on 3 µm thin films of europium-doped Lu_2O_3 in view of possible application in BIPV but the efficiency was strongly limited by scattering losses.[273] Yang et al. have reported a transparent small LSC based on a non-fullerene acceptor molecule as emitter. The absorption onset was at ≈500 nm in a polyacrylic polymer but with substantial overlap of absorption and emission. Thin-film LSCs were fabricated on 26 cm^2 square glass sheet with two edges covered with GaAs PV cells ($G = 4$). The system shows a high optical transmittance of 75% and a PCE of 1.24% with $J_{sc} \approx 2$ mA cm^{-2} but C was largely inferior to unity.[274] Recent work has presented original approaches to light-managing systems combining the specific properties of LSCs with switchability that allows to envision some future advanced light-managing BIVP systems combining controlled transmittance and PV generation.[275–277] Although BIPV is certainly one of the most promising applications of LSCs, work devoted to the realization of systems with dimensions close to real utilization remains scarce, most of the recent work deals with devices of a few square centimeters while LSCs of 100 cm^2 are generally qualified as "large-area LSCs." The fabrication of devices approaching the square meter-scale requires equipment and expertise that largely exceed the capacity of many academic laboratories. However, due to the limitations and poor reliability of results and extrapolations based on miniature devices, the fabrication and evaluation of large-area LSCs appears as a mandatory step towards possible industrial development. Winston and co-workers fabricated plastic LSCs doped with laser dyes and with a maximum size of 60 × 120 cm. With a DR, this system reaches an optical efficiency of 6.6% and $C \approx 4.3$.[278] Li et al. fabricated thin-film LSCs of 30 × 90 cm by doctor blade of colloidal core–shell QDs onto standard window glass, giving C values of ≈0.60.[153] Meinardi and co-workers fabricated 25 × 20 cm plastic LSCs doped with perovskite, with a PCE < 0.50%.[178] More recently, they reported 30 × 30 cm LSCs doped with $CuInS_2$ NCs, leading to an optical power efficiency of 6.8% that is the highest reported to date for a large-area LSCs; however, C is still inferior to unity.[167]

One of the most advanced projects on large-area LSCs for BIVP involves bulk LSCs doped with dyes based on acene and benzothiadiazole compounds developed by ENI. A series of 50 × 50 cm LSCs arranged in modules were tested in real outdoor conditions (**Figure 17**). The LSCs presented a C value of 1.33, an optical efficiency of 6.4%, and a PCE of 1.24%.[279]

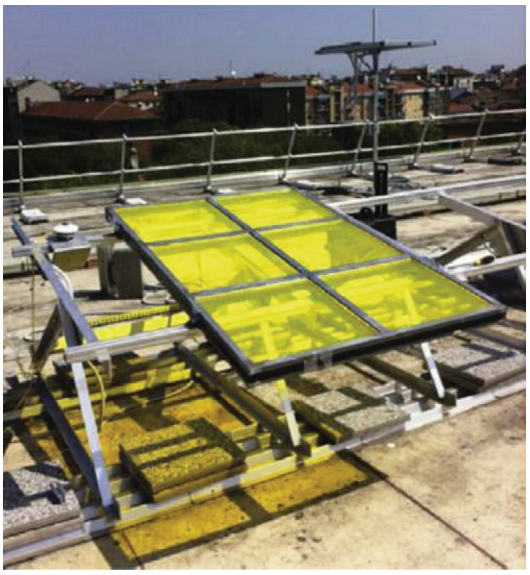

Figure 17. ENI module at the PV test facility of the Politecnico di Milano University. Reproduced with permission.[279] Copyright 2015, Elsevier.

8. Performances of LSCs

As underlined at several instances in this review, the lack of standard definitions of the relevant technical characteristics, performances parameters, and conditions of measurement makes the comparison of the results of the literature quite difficult. In an attempt to present an overview of the state-of-the-art of LSCs performances, the main geometric, optical, and performance characteristics of LSCs are listed in **Tables 1** and **2** in chronological order. Table 1 presents the results published during the early period of LSCs research and Table 2 presents the results corresponding to the "new wave" work. The tables contain exclusively the experimental results obtained under direct full irradiation with simulated or real solar light. Wave-shifters and bottom cell LSCs are not included due to the ambiguity of the definition of G for these systems. Furthermore, such systems are of limited interest in the perspective of BIPV applications. The tables list the input area S, the geometric gain G, the concentration factor C as well as optical and electrical efficiencies when available. When not explicitly indicated in the publication, C is calculated as the product $C = G \times \eta_{opt}$.

Table 1. Characteristics of "old time" LSCs (1977–1987).

Year	S [cm^2]	G	C	η_{opt} [%]	PCE [%]	Emitter	Technology	Ref.
1977	100	83	1.90	2.3		Not defined	Bulk	[13]
	46.3	24	1.50	6.2		Dye	Bulk	
1981	400	33	3.90[a)]	7.5	0.90	Dye	Bulk	[22]
1981	196	12	1.28[a)]	11	2.50	Dye	Bulk	[24]
1981	1200	68	5.10	7.5	1.30	Dye	Bulk	[18]
1982	900	96	2.80[a)]	3.0	0.30	Dye	Bulk	[23]
1984	400	33	3.20	10	1.50	Dye	Bulk	[280]
1984	238	133	9.50[a)]	7.1		Dye	Bulk	[27]
1984	400	130	9.00[a)]	6.9		Dye	Bulk	[30]
1985	2500	16	3.60[a)]	22	2.30	Dye	Bulk	[74]
1987	20	100	2.46[a)]	2.5		Dye	Bulk	[55]
1988	100	8.3	2.98	35.7		Dye	Thin film	[31]

[a)]With a back reflector.

In many studies, C cannot be estimated because of missing experimental detail (dimensions of the device, number of mirrored edges, and conditions of illumination). Due to the dispersity of the dimensions of the devices, direct comparisons should be made with caution; anyway examination of these two sets data allows drawing some obvious conclusions. Early LSCs have much larger area than recent systems. Devices with $S < 100$ cm^2 that were exceptions in the first period are now often qualified as "large-area LSCs" while most of recent work is carried out on devices of a few square centimeters. Consequently, such devices have considerably smaller G values and many devices combine miniature size with $G < 10$. These low G result in very low C values. Thus, while Table 1 shows a lowest C of 1.28 and maximum values of >9, most devices in Table 2 show C values significantly inferior to unity while $C > 1$ are exceptions. Of course, based on the opposite variations of C and η_{opt} versus G, low G values lead to higher efficiencies. The 7.1% efficiency often cited as "world record" corresponds to $C = 0.71$,[62] and it is clear that a reduction of the size and G value of this already small device (25 cm^2) would lead to an even higher efficiency. To summarize, since efficiency is a decreasing function of G it is clear that it cannot be optimized in absolute terms, hence discussing efficiency without reference to S, G, and C does not make sense. On the other hand, since one of the main functions of an LSC is light concentration, it seems evident that C should be always >1. Comparison of the data in both tables clearly shows that whereas early work was focused on the optimization of C, the concentration of solar light is no longer a priority for a majority of recent publications almost exclusively focused on conversion efficiency. However, in most cases, the coupled PV cells produce less electrical energy with a "highly efficient" LSC than without. For a host matrix with refractive index of 1.5, a cubic device of 1 cm with two perpendicular faces as input and output surfaces, an emitter with $\phi_{PL} = 1$, and no reabsorption has a G of 1 a η_{opt} of 0.72 (due to optical losses), and hence $C = 0.72$. Starting from this point that corresponds to the maximum optical efficiency, one has to decide which points of the curves $C = f(G)$ and $\eta_{opt} = f(G)$ are relevant for the envisioned application, keeping in mind that $C > 1$ should be an imperative condition. Of course, many factors must be taken into account to fix S, G, C, and η_{opt}. From a purely economic viewpoint, C could be fixed in order that the reduction of the cost of the PV energy resulting from light concentration covers the extra-cost associated with the insertion of the LSC in a window. This calculation should also take into account the reduced cost of air-conditioning due to light management and consider the annual production of the system since LSCs are relatively more efficient under diffuse light and cloudy weather. However, the application of LSCs in BIPV also involves other factors that are important but difficult to quantify such as aesthetic and artistic aspects.

Table 2. Characteristics of "new wave" LSCs.

Year	S [cm^2]	G	C	η_{opt} [%]	PCE [%]	Emitter	Technology	Ref.
2007	25	16.6	0.29	1.75		Dye	Bulk	[69]
2008	25	2.50	0.71[a)]	28	7.10	Dye	Bulk	[62]
2009	4.0	1.67	0.72[a)]	15.4	6.70	Dye	Bulk	[217]
2011	7200	62.5	**4.23**[a)]	6.6		Dye	Bulk	[278]
2011	15	7.50	**1.91**[a)]	25	2.80	QD	Bulk	[149]
2012	100	10.0	**1.20**	12	1.80	Dye	Bulk	[281]
2013	25	2.50	0.56[a)]	22.6	2.40	Dye	Thin film	[94]
2013	25	2.08	0.87[a)]	42	5.57	None	Bulk	[98]
2014	28	44	0.44[a)]	10.2		QD	Bulk	[67]
2014	1.0	2.50	0.33	13.2		Dye	Thin film	[131]
2015	2500	20.8	**1.33**	6.40	1.24	Dye	Bulk	[279]
2015	144	10	0.33	3.3	3.27	QD	Bulk	[152]
2015	6.25	6.25	0.11	1.8	0.32	Dye	Thin film	[132]
2016	25	2.50	0.80	11.2	3.60	Dye	Bulk	[130]
2016	10.5	23	0.28	1.2	1.20	QD	Bulk	[154]
2016	4.5	10.0	0.61	6.1		QD	Bulk	[272]
2016	412	32.0	0.87	2.7		QD	Thin film	[153]
2016	2.25	3.75	**1.09**	29		Perovskite	Thin film	[183]
2016	25	13.3	0.90	6.8		Dye	Thin film	[120]
2017	56.3	6.7	0.38	5.7		QD	Thin film	[156]
2017	144	11.5	0.33	2.85		QD	Bulk	[158]
2017	4.0	2.5	0.31	12.2	2.63	QD	Bulk	[173]
2017	4.0	2.5	0.19	7.6	1.46	None		[173]
2017	11.7	45	0.90	2.0		Perovskite	Thin film	[179]
2017	25	16.7	**1.23**	7.4		Dye	Thin film	[95]
2017	100	8.30	0.76	9.2	2.44	Dye	Bulk	[128]
2017	500	50.0	0.25	0.50		Perovskite	Bulk	[178]
2017	16.5	55.0	0.80	1.45		Perovskite	Bulk	[179]
2017	4.0	4.90	0.23	4.75		CD	Thin film	[171]
2018	19.8	9.7	0.37	3.7		Dye	Bulk	[113]
2018	100	4	0.30[a)]	8.1	2.94	QD	Bulk	[166]
2018	25	16.7	**1.07**	6.42		Dye	Thin film	[119]
2018	25	13.3	0.93	7.00		Dye	Thin film	[123]
2018	20	9.4	0.35	3.70	0.10	Dye	Thin film	[113]
2018	232	48	**1.70**	3.5	1.10	QD	Thin film	[157]
2018	100	12.5	0.30	2.40		QD	Thin film	[180]
2018	3.0	10	0.12	1.20		CD	Thin film	[170]
2019	3.2	0.9	0.08	4.5		Dye	Bulk	[135]
2019	20.3	3.75	0.19	5.5		Dye	Bulk	[137]
2019	25	16.6	**2.20**[a)]	13.4	2.72	Dye	Bulk	[175]
2019	2.25	1.5	0.45	30		Perovskite		[183]
2019	15	10	0.60	6.0	3.24	Perovskite	Bulk	[185]
2019	100	12.5	0.18	1.44	0.87	Perovskite	Thin film	[186]
2019	5.8	8	0.82	10.3		Dye	Bulk	[226]
2019	100	6.25	0.18	2.95	2.25	QD	Thin film	[162]
2019	900	10.7	0.75	7.4	6.80	QD	Bulk	[167]
2020	56.25	6.25	0.65	10.4	2.20	Dye	Bulk	[138]

[a)]With a back reflector. Data in bold are C values of >1.

9. Conclusion

Forty-five years after the seminal article of Weber and Lambe, the LSC remains an exciting concept that combines simplicity, aesthetic attractiveness, large possibilities of modulation of color, shape transparency, flexibility, low environmental impact, and potential applications in various areas of technological interest. LSCs were initially investigated in view of reducing the cost of PV electricity by concentrating solar light onto expensive PV cells. However, the dramatic drop of the price of PV cells during the past four decades has progressively rendered this motivation obsolete, even if still frequently mentioned in publications. After 20 years of sleep, the renaissance of LSCs occurred in a quite different economic, environmental, and scientific context. As consequences of this long interruption, early research has more or less fallen into oblivion, many concepts recently presented as innovative were in fact already known, while recent literature contains a substantial number of unjustified claims of record performances. Consequently, in spite of a large increase of the number of publications, real advances remain scarce. The concentration factor of LSCs remains a critical issue. This parameter, which was a major objective in early work, is neglected if not completely ignored in many recent articles, whereas most emphasis is placed on conversion efficiency. While high efficiency is of course a priority, this objective should be pursued on devices of size and G values sufficient to ensure C values at least equal to 1. However, because of the opposite variations of concentration and efficiency with the size of the LSC, this change of paradigm has led to a considerable reduction of the average size of the devices investigated with as a consequence that in many "highly efficient" devices, the coupled PV cells produce less electrical energy with the LSC than without. An LSC is expected to fulfill the double function of light conversion and concentration; neglecting one of these two functions in order to optimize the other one does not make great sense. Another problem with miniature devices is that the results and extrapolations based on such devices are questionable due to the irreductible fraction of light guided of scattered independently of any conversion process. In order to remedy these various problems, some recommendations can be proposed. First, it should be underlined that an LSC is a high technology optical system that requires perfect surfaces and meticulous fabrication, implying competences in various disciplines, i.e., chemistry, polymer science, optics, mechanics, and electronics. Insufficient care of these points leads to a serious risk that a nice work on the design of, e.g., advanced emitters, is bungled by the poor quality of the evaluation device. Besides C values generally less than one, very small devices pose serious problems of reliability and a 100 cm^2 input area would be a desirable minimum. When reporting experimental results, all relevant details, namely shape, all dimensions, geometric gain, conditions of illumination, type of PV cells, should be clearly indicated and gathered in the same part of the article. Besides optical and electrical efficiency, the concentration ratio should be always reported and experimental results should be clearly distinct from extrapolated or calculated data. In spite of these problems that could be resolved by cooperative efforts of researchers and journal editors, the renaissance of research on LSCs has produced interesting developments on the passive and active components of LSCs and on the extension of their potential applications. The reduction of optical losses has involved different approaches such as the structuration of the input and output surfaces, the use of band stop filters or selective mirrors, and the orientation of the luminophore. The emitter remains the heart of an LSC and the focus of a major part of research effort. The application of LSCs now essentially oriented towards BIPV has triggered the development of advanced emitters based on various types of NCs such as QDs, CDs, or, more recently, perovskites. These works have led to significant progress in the mitigation of reabsorption and led to the fabrication of several prototypes of LSCs of rather large dimensions that combined optical transparency, no significant spectral distortion of the color perception, and interesting efficiencies, but concentration ratios remain too low. Organic dyes still have potential advantages in terms of tunability of color and emissive properties, processability, and compatibility with polymeric matrixes. While performant large-area LSCs have been fabricated with organic dyes, recent research has led to renewed approaches of FRET, while attempts to take advantage of recent advances in the chemistry of organic luminophores such as AIE or TADF have been reported. These various works show that there is still much room for creative synthetic chemistry. To summarize, while some recent drifts need attention, the LSC remains an exciting concept that will certainly continue to attract much research effort and lead to interesting developments in various areas of photonics.

Acknowledgements

This work was financially supported by the project SMOSCs, ID: 37-220, Cod MySMIS:103509 funded by the Romanian Ministry for European Funds through the National Authority for Scientific Research and Innovation (ANCSI) and co-funded by the European Regional Development Fund/Competitiveness Operational Programme 2014-2020 (POC) Priority Axis 1/Action 1.1.4.

Conflict of Interest

The author declares no conflict of interest.

Keywords

frequency conversion, light concentration, photoluminescence, solar cells

Received: June 10, 2020
Revised: July 24, 2020
Published online: August 6, 2020

[1] W. H. Weber, J. Lambe, *Appl. Opt.* **1976**, *15*, 2299.
[2] A. Goetzberger, W. Greubel, *Appl. Phys.* **1977**, *14*, 123.
[3] B. A. Swartz, T. Cole, A. H. Zewail, *Opt. Lett.* **1977**, *1*, 73.
[4] R. Reisfeld, S. Neuman, *Nature* **1978**, *274*, 144.
[5] A. Goetzberger, *Appl. Phys.* **1978**, *16*, 399.
[6] M. C. Debije, P. P. C. Verbunt, *Adv. Energy Mater.* **2012**, *2*, 12.
[7] F. Meinardi, F. Bruni, S. Brovelli, *Nat. Rev. Mater.* **2017**, *2*, 17072.

[8] G. Keil, *Nucl. Instrum. Methods* **1970**, *89*, 111.
[9] W. G. J. H. M. van Sark, K. W. J. Barnham, L. H. Slooff, A. J. Chatten, A. Büchtemann, A. Meyer, S. J. McCormack, R. Koole, D. J. Farrell, R. Bose, E. E. Bende, A. R. Burgers, T. Budel, J. Quilitz, M. Kennedy, T. Meyer, C. De Mello Donegá, A. Meijerink, D. Vanmaekelbergh, *Opt. Express* **2008**, *16*, 21773.
[10] R. A. S. Ferreira, S. F. H. Correia, A. Monguzzi, X. Liu, F. Meinardi, *Mater. Today* **2020**, *33*, 105.
[11] W. A. Shurcliff, R. C. Jones, *J. Opt. Soc. Am.* **1949**, *39*, 912.
[12] W. A. Shurcliff, *J. Opt. Soc. Am.* **1951**, *41*, 209.
[13] J. A. Levitt, W. H. Weber, *Appl. Opt.* **1977**, *16*, 2684.
[14] A. Goetzberger, *Sol. Energy* **1979**, *22*, 435.
[15] J. S. Batchelder, A. H. Zewail, T. Cole, *Appl. Opt.* **1979**, *18*, 3090.
[16] R. Reisfeld, Y. Kalisky, *Nature* **1980**, *283*, 281.
[17] E. Yablonovitch, *J. Opt. Soc. Am.* **1980**, *70*, 1362.
[18] J. S. Batchelder, A. H. Zewail, T. Cole, *Appl. Opt.* **1981**, *20*, 3733.
[19] R. W. Olson, R. F. Loring, M. D. Fayer, *Appl. Opt.* **1981**, *20*, 2934.
[20] J. Sansregret, J. M. Drake, W. R. L. Thomas, M. L. Lesiecki, *Appl. Opt.* **1983**, *22*, 573.
[21] W. R. L. Thomas, J. M. Drake, M. L. Lesiecki, *Appl. Opt.* **1983**, *22*, 3440.
[22] K. Heidler, *Appl. Opt.* **1981**, *20*, 773.
[23] J. M. Drake, M. L. Lesiecki, J. Sansregret, W. R. L. Thomas, *Appl. Opt.* **1982**, *21*, 2945.
[24] P. S. Friedman, *Opt. Eng.* **1981**, *6*, 887.
[25] A. Filloux, J. Mugnier, B. V. Bourson, *Rev. Phys. Appl.* **1983**, *18*, 273.
[26] G. Lifante, F. Cusso, F. Meseguer, F. Jaque, *Appl. Opt.* **1983**, *22*, 3966.
[27] J. Roncali, F. Garnier, *Appl. Opt.* **1984**, *23*, 2809.
[28] E. LohJr., D. J. Scalapino, *Appl. Opt.* **1986**, *25*, 1901.
[29] G. Smestad, P. Hamill, *Appl. Opt.* **1984**, *23*, 4394.
[30] J. Roncali, F. Garnier, *Sol. Cells* **1984**, *13*, 133.
[31] R. Reisfeld, M. Eyal, V. Chernyak, R. Zusman, *Sol. Energy Mater. Sol. Cells* **1988**, *17*, 439.
[32] H. Ma, A.-K. Y. Jen, L. R. Dalton, *Adv. Mater.* **2002**, *14*, 1339.
[33] R. Ross, *J. Chem. Phys.* **1967**, *46*, 4590.
[34] E. Yablonovitch, *J. Opt. Soc. Am.* **1980**, *70*, 1362.
[35] A. Lempicki, *Appl. Opt.* **1983**, *22*, 1160.
[36] G. Smestad, H. Ries, R. Winston, E. Yablonovitch, *Sol. Energy Mater. Sol. Cells* **1990**, *21*, 99.
[37] K. Barnham, J. L. Marques, J. Hassard, P. O'Brien, *Appl. Phys. Lett.* **2000**, *76*, 1197.
[38] A. A. Earp, G. B. Smith, P. D. Swift, J. Franklin, *Sol. Energy* **2004**, *76*, 655.
[39] U. Rau, F. Einsele, G. C. Glaeser, *Appl. Phys. Lett.* **2005**, *87*, 171101.
[40] P. F. Scudo, L. Abbondanza, R. Fusco, L. Caccianotti, *Sol. Energy Mater. Sol. Cells* **2010**, *94*, 1241.
[41] G. C. Glaeser, U. Rau, *Proc. SPIE* **2006**, *6197*, 61970L.
[42] S. McDowall, B. L. Johnson, D. L. Patrick, *J. Appl. Phys.* **2010**, *108*, 053508.
[43] S. W. Leow, C. Corrado, M. Osborn, S. A. Carter, *Proc. SPIE* **2013**, *8821*, 882103.
[44] A.-L. Joudrier, F. Proise, R. Grapina, J.-L. Pelouard, J.-F. Guillemoles, *Energy Procedia* **2014**, *60*, 173.
[45] T. S. Parel, C. Pistolas, L. Danos, T. Markvart, *Opt. Mater.* **2015**, *42*, 532.
[46] F. Proise, A.-L. Joudrier, J.-L. Pelouard, J.-F. Guillemoles, *EPJ Photovoltaics* **2018**, *9*, 12.
[47] C. Yang, D. Liu, R. Lunt, *Joule* **2019**, *3*, 2871.
[48] M. L. Lesiecki, J. Michael Drake, *Appl. Opt.* **1982**, *21*, 557.
[49] S. M. Reda, *Dyes Pigm.* **2007**, *75*, 526.
[50] M. G. Debije, P. P. C. Verbunt, B. C. Rowan, B. S. Richards, T. L. Hoeks, *Appl. Opt.* **2008**, *47*, 6763.
[51] J. C. Goldschmidt, M. Peters, M. Hermle, S. W. Glunz, *J. Appl. Phys.* **2009**, *105*, 114911.
[52] C. Tummeltshammer, A. Taylor, A. J. Kenyon, I. Papakonstantinou, *Sol. Energy Mater. Sol. Cells* **2016**, *144*, 40.
[53] A. Budó, I. Ketskeméty, *J. Chem. Phys.* **1956**, *25*, 595.
[54] R. Soti, E. Farkas, M. Hilbert, Z. S. Farkas, I. Ketskemety, *J. Lumin.* **1995**, *63*, 251.
[55] J. Mugnier, Y. Dordet, J. Pouget, M. T. Le Bris, B. Valeur, *Sol. Energy Mater. Sol. Cells* **1987**, *15*, 65.
[56] E. J. Nunes Pereira, M. N. Berberan-Santos, J. M. G. Martinho, *J. Lumin.* **1995**, *63*, 258.
[57] T. Dienel, C. Bauer, I. Dolamic, D. Brühwiler, *Sol. Energy* **2010**, *84*, 1366.
[58] L. Fang, T. S. Parel, L. Danos, T. Markvart, *J. Appl. Phys.* **2012**, *111*, 706104.
[59] L. R. Wilson, B. C. Rowan, N. Robertson, O. Moudam, A. C. Jones, B. S. Richards, *Appl. Opt.* **2010**, *49*, 1651.
[60] Z. Krumer, W. G. J. H. M. van Sark, C. de Mello Donega, R. E. I. Schropp, *Proc. SPIE* **2013**, *8821*, 882104.
[61] C. Yang, J. Zhang, W.-T. Peng, W. Sheng, D. Liu, P. S. Kuttipillai, M. Young, M. R. Donahue, B. G. Levine, B. Borhan, R. R. Lunt, *Sci. Rep.* **2018**, *8*, 1635.
[62] L. H. Slooff, E. E. Bende, A. R. Burgers, T. Budel, M. Pravettoni, R. P. Kenny, E. D. Dunlop, A. Büchtemann, *Phys. Status Solidi* **2008**, *2*, 257.
[63] M. Sidrach de Cardona, M. Carrascosa, F. Meseguer, F. Cusso, F. Jaque, *Sol. Cells* **1985**, *15*, 225.
[64] R. Reisfeld, D. Shamrakov, C. Jorgensen, *Sol. Energy Mater. Sol. Cells* **1994**, *33*, 417.
[65] M. J. Currie, J. K. Mapel, T. D. heidel, S. Goffri, M. A. Baldo, *Science* **2008**, *321*, 226.
[66] I. Coropceanu, M. G. Bawendi, *Nano Lett.* **2014**, *14*, 4097.
[67] F. Meinardi, A. Colombo1, K. A. Velizhanin, R. Simonutti, M. Lorenzon, L. Beverina, R. Viswanatha, V. I. Klimov, S. Brovelli, *Nat. Photonics* **2014**, *8*, 392.
[68] S. F. H. Correia, P. P. Lim, P. S. André, M. R. Sá Ferreira, L. A. Dias Carlos, *Sol. Energy Mater. Sol. Cells* **2015**, *138*, 51.
[69] S. J. Gallagher, B. Norton, P. C. Eames, *Sol. Energy* **2007**, *81*, 813.
[70] N. D. Bronstein, Y. Yao, L. Xu, L. O'Brien, A. S. Powers, V. E. Ferry, A. P. Alivisatos, R. G. Nuzzo, *ACS Photonics* **2015**, *2*, 1576.
[71] H.-J. Song, B. G. Jeong, J. Lim, D. C. Lee, W. K. Bae, V. I. Klimov, *Nano Lett.* **2018**, *18*, 395.
[72] Y. Li, X. Zhang, Y. Zhang, R. Dong, C. K. Luscombe, *J. Polym. Sci., Part A: Polym. Chem.* **2019**, *57*, 201.
[73] G. Griffini, *Front. Mater.* **2019**, *6*, 29.
[74] M. Sidrach de Cardona, M. Carrascosa, F. Meseguer, F. Cusso, F. Jaque, *Appl. Opt.* **1985**, *24*, 2028.
[75] A. F. Mansour, *Polym. Test.* **1998**, *17*, 153.
[76] V. Sholin, J. D. Olson, S. A. Carter, *J. Appl. Phys.* **2007**, *101*, 123114.
[77] C. L. Mulder, L. Theogarajan, M. Currie, J. K. Mapel, M. A. Baldo, M. Vaughn, P. Willard, B. D. Bruce, M. W. Moss, C. E. McLain, J. P. Morseman, *Adv. Mater.* **2009**, *21*, 3181.
[78] G. V. Shcherbatyuk, R. H. Inman, C. Wang, R. Winston, S. Gosh, *Appl. Phys. Lett.* **2010**, *96*, 191901.
[79] C. Tummeltshammer, M. Portnoi, S. A. Mitchell, A.-T. Lee, A. J. Kenyon, A. B. Tabor, I. Papakonstantinou, *Nano Energy* **2017**, *32*, 263.
[80] M. Gajic, F. Lisi, N. Kirkwood, T. A. Smith, P. Mulvaney, G. Rosengarten, *Sol. Energy* **2017**, *150*, 30.
[81] Z. Krumer, W. G. J. H. M. van Sark, R. E. I. Schropp, C. de Mello Donegá, *Sol. Energy Mater. Sol. Cells* **2017**, *167*, 133.
[82] X. Liu, B. Luo, J. Liu, D. Jing, D. Benetti, F. Rosei, *J. Mater. Chem. A.* **2020**, *8*, 1787.
[83] R. Reisfled, N. Manor, D. Avnir, *Sol. Energy Mater. Sol. Cells* **1983**, *8*, 399.
[84] G. Folcher, N. Keller, J. Paris, *Sol. Energy Mater. Sol. Cells* **1984**, *10*, 303.

[85] B. Jezowska-Trzebiatowska, E. Lukowiak, W. Strik, A. Buczkowsli, S. Patela, J. Radojewski, *Sol. Energy Mater. Sol. Cells* **1986**, *13*, 267.
[86] S. M. Reda, *Dyes Pigm.* **2007**, *75*, 526.
[87] M. J. Kastelijn, C. W. M. Bastiaansen, M. G. Debije, *Opt. Mater.* **2009**, *31*, 1720.
[88] V. Fattori, M. Melucci, L. Ferrante, M. Zambianchi, I. Manet, W. Oberhauser, G. Giambastiani, M. Frediani, G. Giachi, N. Camaioni, *Energy Environ. Sci.* **2011**, *4*, 2849.
[89] S. M. El Bashir, *J. Lumin.* **2012**, *132*, 1786.
[90] Y. S. Lim, C. K. Lo, G. B. Teh, *Renewable Energy* **2012**, *45*, 156.
[91] M. Melucci, M. Durso, L. Favaretto, M. L. Capobianco, V. Benfenati, A. Sagnella, G. Ruani, M. Muccini, R. Zamboni, V. Fattori, N. Camaioni, *RSC Adv.* **2012**, *2*, 8610.
[92] G. Griffini, M. Levi, S. Turri, *Sol. Energy Mater. Sol. Cells* **2013**, *118*, 36.
[93] G. Griffini, M. Levi, S. Turri, *Prog. Org. Coat.* **2014**, *77*, 528.
[94] G. Maggioni, A. Campagnaro, S. Carturan, A. Quaranta, *Sol. Energy Mater. Sol. Cells* **2013**, *108*, 27.
[95] M. Sottile, G. Tomei, S. Borsacchi, F. Martini, M. Geppi, G. Ruggeri, A. Pucci, *Eur. Polym. J.* **2017**, *89*, 23.
[96] E. Tatsi, G. Fortunato, B. Rigatelli, G. Lyu, S. Turri, R. C. Evans, G. Griffini, *ACS Appl. Energy Mater.* **2020**, *3*, 1152.
[97] M. Buffa, S. Carturan, M. G. Debije, A. Quaranta, G. Maggioni, *Sol. Energy Mater. Sol. Cells* **2012**, *103*, 114.
[98] C.-H. Chou, J.-K. Chuang, F.-C. Chen, *Sci. Rep.* **2013**, *3*, 2244.
[99] C.-H. Chou, M.-H. Hsu, F. C. Chen, *Nano Energy* **2015**, *15*, 729.
[100] S. F. H. Correia, P. P. Lima, E. P. Sidney, J. L. Ribeiro, P. S. André Rute, A. S. Ferreira, L. D. Carlos, *Prog. Photovoltaics* **2016**, *24*, 1178.
[101] X.-H. Hu, J.-D. Liu, X. Y. Du, R. Cheng, Q. Li, S. Chen, *J. Mater. Chem. C* **2019**, *7*, 10988.
[102] K. K. Pandey, T. C. Pant, *Sol. Energy Mater. Sol. Cells* **1991**, *21*, 327.
[103] J. Sathian, J. D. Breeze, B. Richards, N. M. Alford, M. Oxborrow, *Opt. Express* **2017**, *25*, 13714.
[104] W. Wu, T. Wang, X. Wang, S. Wu, Y. Luo, X. Tian, Q. Zhang, *Sol. Energy* **2010**, *84*, 2140.
[105] D. K. G. de Boer, D. J. Broer, M. G. Debije, W. Keur, A. Meijerink, C. R. Ronda, P. P. C. Verbunt, *Opt. Express* **2012**, *20*, A395.
[106] Y. Zhao, R. R. Lunt, *Adv. Energy Mater.* **2013**, *3*, 1143.
[107] V. T. Freitas, L. Fu, A. M. Cojocariu, X. Cattoe, J. R. Bartlett, R. Le Parc, J.-L. Bantignies, M. Wong Chi Man, P. S. Andre, R. A. S. Ferreira, L. D. Carlos, *ACS Appl. Mater. Interfaces* **2015**, *7*, 8770.
[108] A. R. Frias, M. A. Cardoso, A. R. N. Bastos, S. F. H. Correia, P. S. André, L. D. Carlos, V. de Zea Bermudez, R. A. S. Ferreira, *Energies* **2019**, *12*, 451.
[109] H.-Y. Huang, K.-B. Cai, P.-W. Chen, C.-A. J. Lin, S.-H. Chang, C.-T. Yuan, *J. Phys. Chem. C* **2018**, *122*, 20019.
[110] J. Mei, N. L. C. Leung, R. T. K. Kwok, J. W. Y. Lam, B. Z. Tang, *Chem. Rev.* **2015**, *115*, 11718.
[111] Y. Tao, K. Yuan, T. Chen, P. Xu, H. H. Li, R. Chen, C. Zheng, L. Zhang, W. Huang, *Adv. Mater.* **2014**, *26*, 7931.
[112] G. Seybold, G. Wagenblast, *Dyes Pigm.* **1989**, *11*, 303.
[113] A. R. Frias, E. Pecoraro, S. F. H. Correia, L. M. G. Minas, A. R. Bastos, S. Garcıa-Revilla, R. Balda, S. J. L. Ribeiro, P. S. Andre, L. D. Carlos, R. A. S. Ferreira, *J. Mater. Chem. A* **2018**, *6*, 8712.
[114] S. Sadeghi, R. Melikov, H. B. Jalali, O. Karatum, S. B. Srivastava, D. Conkar, E. N. F. Karalar, S. Nizamoglu, *ACS Appl. Mater. Interfaces* **2019**, *11*, 8710.
[115] T. Saraidarov, V. Levchenko, A. Grabowska, P. Borowicz, R. Reisfeld, *Chem. Phys. Lett.* **2010**, *492*, 60.
[116] M. G. Debije, P. P. C. Verbunt, P. J. Nadkarni, S. Velate, K. Bhaumik, S. Nedumbamana, B. C. Rowan, B. S. Richards, T. L. Hoeks, *Appl. Opt.* **2011**, *50*, 163.
[117] R. Turrisi, A. Sanguineti, M. Sassi, B. Savoie, A. Takai, G. E. Patriarca, M. M. Salamone, R. Ruffo, G. Vaccaro, F. Meinardi, T. J. Marks, A. Facchetti, L. Beverina, *J. Mater. Chem. A* **2015**, *3*, 8045.
[118] A. Sanguineti, M. Sassi, R. Turrisi, R. Ruffo, G. V. F. Meinardi, L. Beverina, *Chem. Commun.* **2013**, *49*, 1618.
[119] C. Papucci, T. A. Geervliet, D. Franchi, O. Bettucci, A. Mordini, G. Reginato, F. Picchioni, A. Pucci, M. Calamante, L. Zani, *Eur. J. Org. Chem.* **2018**, *2018*, 2657.
[120] J. Lucarelli, M. Lessi, C. Manzini, P. Minei, F. Bellina, A. Pucci, *Dyes Pigm.* **2016**, *135*, 154.
[121] G. Albano, T. Colli, L. Nucci, R. Charaf, T. Biver, A. Pucci, L. A. Aronica, *Dyes Pigm.* **2020**, *174*, 108100.
[122] P. Della Sala, N. Buccheri, A. Sanzone, M. Sassi, P. Neri, C. Talotta, A. Rocco, V. Pinchetti, L. Beverina, S. Brovelli, C. Gaeta, *Chem. Commun.* **2019**, *55*, 3160.
[123] G. Marianetti, M. Lessi, V. Barone, F. Bellina, A. Pucci, *Dyes Pigm.* **2018**, *157*, 334.
[124] B. Balaban, S. Doshay, M. Osborn, Y. Rodriguez, S. A. Carter, *J. Lumin.* **2014**, *146*, 256.
[125] G. D. Gutierrez, I. Coropceanu, M. G. Bawendi, T. M. Swager, *Adv. Mater.* **2016**, *28*, 497.
[126] O. A. Bozdemir, S. Erbas-Cakmak, O. O. E. A. Dana, U. Akkaya, *Angew. Chem., Int. Ed.* **2011**, *50*, 10907.
[127] A. Mirloup, P. Retailleau, R. Ziessel, *Tetrahedron Lett.* **2013**, *54*, 4456.
[128] N. J. L. K. Davis, R. W. MacQueen, S. T. E. Jones, C. Orofino-Pena, D. Cortizo-Lacalle, R. G. D. Taylor, D. Credgington, P. J. Skabara, N. C. Greenham, *J. Mater. Chem. C* **2017**, *5*, 1952.
[129] S. T. Bailey, G. E. Lokey, M. S. Hanes, J. D. M. Shearer, J. B. McLafferty, G. T. Beaumont, T. T. Baseler, J. M. Layhue, D. R. Broussard, Y.-Z. Zhang, B. P. Wittmershaus, *Sol. Energy Mater. Sol. Cells* **2007**, *91*, 67.
[130] A. L. Martínez, D. Gómez, *J. Photonics Energy* **2016**, *6*, 045504.
[131] J. L. Banal, J. M. White, K. P. Ghiggino, W. W. H. Wong, *Sci. Rep.* **2015**, *4*, 4635.
[132] J. L. Banal, J. M. White, T. W. Lam, A. W. Blakers, K. P. Ghiggino, W. W. H. Wong, *Adv. Energy Mater.* **2015**, *5*, 1500818.
[133] J. L. Banal, K. P. Ghiggino, W. W. H. Wong, *Phys. Chem. Chem. Phys.* **2014**, *16*, 25358.
[134] J. L. Banal, B. Zhang, D. J. Jones, K. P. Ghiggino, W. W. H. Wong, *Acc. Chem. Res.* **2017**, *50*, 49.
[135] W. Ma, W. Lia, M. Cao, R. Liu, X. Zhao, X. Gong, *Org. Electron.* **2019**, *73*, 226.
[136] A. Pucci, *Isr. J. Chem.* **2018**, *58*, 837.
[137] G. Lyu, J. Kendall, I. Meazzini, E. Preis, S. Bayseç, U. Scherf, S. Clément, R. C. Evans, *ACS Appl. Polym. Mater.* **2019**, *1*, 3039.
[138] F. Mateen, S. Y. Lee, S.-K. Hong, *J. Mater. Chem. A* **2020**, *8*, 3708.
[139] A. P. Alivisatos, *Science* **1996**, *271*, 933.
[140] F. Purcell-Milton, Y. K. Gun'ko, *J. Mater. Chem.* **2012**, *22*, 16687.
[141] H. Zhao, F. Rosei, *Chem* **2017**, *3*, 227.
[142] H. Z. Zhou, D. Ma, F. Rosei, *Chem. Soc. Rev.* **2018**, *47*, 5866.
[143] P. Moraitis, R. E. I. Schropp, W. G. J. H. M. van Sark, *Opt. Mater.* **2018**, *84*, 636.
[144] R. Mazzaro, A. Vomiero, *Adv. Energy Mater.* **2018**, *8*, 1801903.
[145] K. Barnham, J. L. Marques, J. Hassard, P. O'Brien, *Appl. Phys. Lett.* **2000**, *76*, 1197.
[146] A. J. K. Chatten, W. J. Barnham, B. F. Buxton, N. J. Ekins-Daukes, M. Malik, *Sol. Energy Mater. Sol. Cells* **2003**, *75*, 363.
[147] A. J. K. Chatten, W. J. Barnham, B. F. Buxton, N. J. Ekins-Daukes, M. Malik, *Sol. Energy Mater. Sol. Cells* **2004**, *38*, 909.
[148] M. G. Hyldahl, S. T. Bailey, B. P. Wittmershaus, *Sol. Energy* **2009**, *83*, 566.
[149] J. Bomm, A. Büchtemann, A. J. Chatten, R. Bose, D. J. Farrell, N. L. A. Chan, Y. Xiao, L. H. Slooff, T. Meyer, A. Meyer, W. G. J. H. M. van Sark, R. Koole, *Sol. Energy Mater. Sol. Cells* **2011**, *95*, 2087.

[150] Z. Krumer, S. J. Pera, R. J. A. van Dijk-Moes, Y. Zhao, A. F. P. de Brouwer, E. Groeneveld, W. G. J. H. M. van Sark, R. E. I. Schropp, C. de Mello Donega, *Sol. Energy Mater. Sol. Cells* **2013**, *111*, 57.
[151] C. S. Erickson, L. R. Bradshaw, S. McDowall, J. D. Gilbertson, D. R. Gamelin, D. L. Patrick, *ACS Nano* **2014**, *8*, 3461.
[152] F. Meinardi, H. McDaniel, F. Carulli, A. Colombo, K. A. Velizhanin, N. S. Makarov, R. Simonutti, V. Klimov, S. Brovelli, *Nat. Nanotechnol.* **2015**, *10*, 878.
[153] H. Li, K. Wu, J. Lim, H.-J. Song, V. I. Klimov, *Nat. Energy* **2016**, *1*, 16157.
[154] H. Zao, D. Benetti, L. Jin, Y. Zhou, F. Rosei, A. Vomiero, *Small* **2016**, *12*, 5354.
[155] L. Tan, Y. Zhou, F. Ren, D. Benetti, F. Yang, H. Zhao, F. Rosei, M. Chaker, D. Ma, *J. Mater. Chem. A* **2017**, *5*, 10250.
[156] R. Sumner, S. Eiselt, T. B. Kilburn, C. Erickson, B. Carlson, D. R. Gamelin, S. McDowall, D. L. Patrick, *J. Phys. Chem. C* **2017**, *121*, 3252.
[157] K. Wu, H. Li, V. I. Klimov, *Nat. Photonics* **2018**, *12*, 105.
[158] F. Meinardi, S. Ehrenberg, L. Dhamo, F. Carulli, M. Mauri, F. Bruni, R. Simonutti, U. Kortshagen, S. Brovelli, *Nat. Photonics* **2017**, *11*, 177.
[159] H. Liu, S. Li, W. Chen, D. Wang, C. Li, D. Wu, J. Hao, Z. Zhou, X. Wang, K. Wang, *Sol. Energy Mater. Sol. Cells* **2018**, *179*, 380.
[160] S. K. E. Hill, R. Connell, C. Peterson, J. Hollinger, M. A. Hillmyer, U. Kortshagen, V. E. Ferry, *ACS Photonics* **2019**, *6*, 170.
[161] G. Liu, H. Zhao, F. Diao, Z. Ling, Y. Wang, *J. Mater. Chem. C* **2018**, *6*, 10059.
[162] G. Liu, R. Mazzaro, Y. Wang, H. Zhao, A. Vomiero, *Nanoenergy* **2019**, *60*, 119.
[163] R. Mazzaro, A. Gradone, S. Angeloni, G. Morselli, P. G. Cozzi, F. Romano, A. Vomiero, P. Ceroni, *ACS Photonics* **2019**, *6*, 2303.
[164] S. K. E. Hill, R. Connell, J. Held, C. Peterson, M. A. H. Francis, V. E. Ferry, U. Kortshagen, *ACS Appl. Mater. Interfaces* **2020**, *12*, 4572.
[165] J. Wang, Y. Yuan, H. Zhu, T. Cai, Y. Fang, O. Chen, *Nano Energy* **2020**, *67*, 104217.
[166] M. R. Bergren, N. S. Makarov, K. Ramasamy, A. Jackson, R. Guglielmetti, H. McDaniel, *ACS Energy Lett.* **2018**, *3*, 520.
[167] A. Anand, M. L. Zaffalon, G. Gariano, A. Camellini, M. Gandini, R. Brescia, C. Capitani, F. Bruni, V. Pinchetti, M. Zavelani-Rossi, F. Meinardi, S. A. Crooker, S. Brovelli, *Adv. Funct. Mater.* **2020**, *30*, 1906629.
[168] Z. Li, X. Zhao, C. Huang, X. Gong, *J. Mater. Chem. C* **2019**, *7*, 12373.
[169] Y. Zhou, D. Benetti, X. Tong, L. Jin, Z. M. Wang, D. Ma, H. Zhao, F. Rosei, *Nano Energy* **2018**, *44*, 378.
[170] M. J. Talite, H.-Y. Huang, Y.-H. Wu, P. G. Sena, K.-B. Cai, T.-N. Lin, J.-L. Shen, W.-C. Chou, C.-T. Yuan, *Appl. Mater. Interfaces* **2018**, *10*, 34184.
[171] Y. Li, P. Miao, W. Zhou, X. Gong, X. Zhao, *J. Mater. Chem. A* **2017**, *5*, 21452.
[172] Z. Wang, X. Zhao, Z. Guo, P. Miao, X. Gong, *Org. Electron.* **2018**, *62*, 284.
[173] X. Gong, W. Ma, Y. Li, L. Zhong, W. Li, X. Zhao, *Org. Electron.* **2018**, *63*, 237.
[174] W. Ma, W. Li, R. Liu, M. Cao, X. Zhao, X. Gong, *Chem. Commun.* **2019**, *55*, 7486.
[175] F. Mateen, M. Ali, S. Y. Lee, S. H. Jeong, M. J. Ko, S.-K. Hong, *Sol. Energy* **2019**, *190*, 488.
[176] M. J. Talite, H.-Y. Huang, K.-B. Cai, K. C. Capinig Co, P. A. C. Santoso, S.-H. Chang, W.-C. Chou, C.-T. Yuan, *J. Phys. Chem. Lett.* **2020**, *11*, 567.
[177] S. Mirershadi, S. Ahmadi-Kandjani, *Dyes Pigm.* **2015**, *120*, 15.
[178] F. Meinardi, Q. A. Akkerman, F. Bruni, S. Park, M. Mauri, Z. Dang, L. Manna, S. Brovelli, *ACS Energy Lett.* **2017**, *2*, 2368.
[179] H. Zhao, Y. Zhou, D. Benettia, D. Ma, F. Rosei, *Nano Energy* **2017**, *37*, 214.
[180] H. Zhao, D. Benetti, X. Tong, H. Zhang, Y. Zhou, G. Liu, D. Ma, S. Sun, Z. M. Wang, Y. Wang, F. Rosei, *Nano Energy* **2018**, *50*, 756.
[181] K. Luo, T. Ding, X. Liu, Y. Liu, K. Wu, *Nano Lett.* **2019**, *19*, 338.
[182] J. Tong, J. Luo, L. Shi, J. Wu, L. Xu, J. Song, P. Wang, H. Li, Z. Deng, *J. Mater. Chem. A* **2019**, *7*, 4872.
[183] K. Nikolaidou, S. Sarang, C. Hoffman, B. Mendewala, H. Ishihara, J. Q. Lu, B. Ilan, V. Tung, S. Ghosh, *Adv. Opt. Mater.* **2016**, *4*, 2126.
[184] B. Mendewala, K. Nikolaidou, C. Hoffman, S. Saranga, J. Luc, B. Ilan, S. Ghosh, *Sol. Energy* **2019**, *183*, 392.
[185] E. Bagherzadeh-Khajehmarjana, A. Nikniazia, B. Olyaeefara, S. Ahmadi-Kandjania, J.-M. Nunzi, *Sol. Energy Mater. Sol. Cells* **2019**, *192*, 44.
[186] M. Wei, F. Pelayo García de Arquer, G. Walters, Z. Yang, L. N. Quan, Y. Kim, R. Sabatini, R. Quintero-Bermudez, L. Gao, J. Z. Fan, F. Fan, A. Gold-Parker, M. F. Toney, E. H. Sargent, *Nat. Energy* **2019**, *4*, 197.
[187] H. J. Hovel, R. T. Hogson, J. M. Woodall, *Sol. Energy Mater. Sol. Cells* **1979**, *2*, 19.
[188] W. Viehmann, R. L. Frost, *Nucl. Instrum. Methods* **1979**, *167*, 405.
[189] D. Sarti, F. LePoull, Ph. Gravisse, *Sol. Cells* **1981**, *4*, 25.
[190] W. G. J. H. M. van Sark, A. Meijerink, R. E. I. Schropp, J. A. M. van Roosmalen, E. H. Lysen, *Sol. Energy Mater. Sol. Cells* **2005**, *87*, 395.
[191] B. S. Richards, *Sol. Energy Mater. Sol. Cells* **2006**, *90*, 2329.
[192] E. Klampaftis, D. Ross, K. R. McIntosh, B. S. Richards, *Sol. Energy Mater. Sol. Cells* **2009**, *93*, 1182.
[193] J. Day, S. Senthilarasu, T. K. Mallick, *Sol. Energy Mater. Sol. Cells* **2019**, *199*, 83.
[194] C. Corrado, S. W. Leow, M. Osborn, E. Chan, B. Balaban, S. A. Carter, *Sol. Energy Mater. Sol. Cells* **2013**, *111*, 74.
[195] S. W. Leow, C. Corrado, M. Osborn, M. Isaacson, G. Alers, S. A. Carter, *J. Appl. Phys.* **2013**, *113*, 214510.
[196] Y. Zhang, S. Sun, R. Kang, J. Zhang, N. Zhang, W. Yan, W. Xie, J. Ding, J. Bao, C. Gao, *Energy Convers. Manage.* **2015**, *95*, 187.
[197] W. Zhou, M.-C. Wang, X. Zhao, *Sol. Energy* **2015**, *120*, 419.
[198] S. Chandra, M. Rafiee, J. Doran, S. J. Mc Cormack, *Sol. Energy Mater. Sol. Cells* **2018**, *182*, 331.
[199] R. Soti, E. Farkas, M. Hilbert, Zs. Farkas, I. Ketskemkty, *J. Lumin.* **1996**, *68*, 105.
[200] B. Vishwanathan, A. H. M. E. Reinders, D. K. G. de Boer, L. Desmet, A. J. M. Ras, F. H. Zahn, M. G. Debije, *Sol. Energy* **2015**, *112*, 120.
[201] K. R. McIntosh, N. Yamada, B. S. Richards, *Appl. Phys. B* **2007**, *88*, 285.
[202] C. Wang, H. Abdul-Rahman, S. P. Rao, *Int. J. Energy Res.* **2010**, *34*, 1372.
[203] R. H. Inman, G. V. Shcherbatyuk, D. Medvedko, A. Gopinathan, S. Ghosh, *Opt. Express* **2011**, *19*, 24308.
[204] I. Parola, D. Zaremba, R. Evert, J. Kielhorn, F. Jakobs, M. A. Illarramendi, J. Zubiac, W. Kowalsky, H. H. Johannes, *Sol. Energy Mater. Sol. Cells* **2018**, *178*, 20.
[205] F. Mateen, H. Oh, J. Kang, S. Y. Lee, S. K. Hong, *Renewable Energy* **2019**, *138*, 691.
[206] A. Goetzberger, O. Schirmer, *Appl. Phys.* **1979**, *19*, 5358.
[207] N. C. Giebink, *Proc. SPIE* **2011**, *8438*, 84380V1.
[208] S. Tsoi, D. J. Broer, C. W. M. Bastiaansen, M. G. Debije, *Opt. Express* **2010**, *18*, A536.
[209] P. T. M. Albers, C. W. M. Bastiaansen, M. G. Debije, *Sol. Energy* **2013**, *95*, 216.
[210] N. C. Giebink, G. P. Wiederrecht, R. R. Wasielewski, *Nat. Photonics* **2011**, *5*, 694.
[211] S. Tsoi, D. J. Broer, C. W. M. Bastiaansen, M. G. Debije, *Adv. Energy Mater.* **2013**, *3*, 337.
[212] M. D. Hughes, C. Maher, D.-A. Borca-Tasciuc, D. Polanco, D. Kaminski, *Renewable Energy* **2013**, *52*, 266.

[213] Y. Shen, Y. Jia, X. Sheng, L. Shen, J. A. Rogers, N. C. Giebink, *ACS Photonics* **2014**, *1*, 746.
[214] G. Lifante, F. Cusso, F. Messeguer, F. Jaque, *Sol. Cells* **1983**, *8*, 355.
[215] M. Kennedy, S. J. McCormack, J. Doran, B. Norton, *Proc. SPIE* **2007**, *6649*, 664905.
[216] M. G. Debije, J. P. Teunissen, M. J. Kastelijn, P. P. C. Verbunt, C. W. M. Bastiaansen, *Sol. Energy Mater. Sol. Cells* **2009**, *93*, 1345.
[217] J. C. Goldschmidt, M. Peters, A. Bosch, H. Helmers, F. Dimroth, S. W. Glunz, G. Willeke, *Sol. Energy Mater. Sol. Cells* **2009**, *93*, 176.
[218] M. G. Debije, W. Dekkers, *J. Renewable Sustainable Energy* **2012**, *4*, 013103.
[219] J. R. Schrecengost, S. D. Bowser, S. W. Weible, J. M. Solomon, L. J. Minner, J. T. Gresh, B. P. Wittmershaus, *Sol. Energy* **2018**, *170*, 132.
[220] D. J. Farrell, M. Yoshida, *Prog. Photovoltaics* **2012**, *20*, 93.
[221] J. C. Goldschmidt, M. Peters, L. Prönneke, L. Steidl, R. Zentel, B. Bläsi, A. Gombert, S. Glunz, G. Willeke, U. Rau, *Phys. Status Solidi* **2008**, *205*, 2811.
[222] M. G. Debije, M.-P. Van, P. P. C. Verbunt, M. J. Kastelijn, R. H. L. van der Blom, D. J. Broer, C. W. M. Bastiaansen, *Appl. Opt.* **2010**, *49*, 745.
[223] D. K. G. de Boer, C.-W. Lin, M. P. Giesbers, H. J. Cornelissen, M. G. Debije, P. P. C. Verbunt, D. J. Broer, *Appl. Phys. Lett.* **2011**, *98*, 021111.
[224] A.-L. Joudrier, F. Proise, R. Grapin, J.-L. Pelouard, J.-F. Guillemoles, *Energy Procedia* **2014**, *60*, 173.
[225] L. Xu, Y. Yao, N. D. Bronstein, L. Li, A. P. Alivisatos, R. G. Nuzzo, *ACS Photonics* **2016**, *3*, 278.
[226] G. Iasilli, R. Francischello, P. Lova, S. Silvano, A. Surace, G. Pesce, M. Alloisio, M. Patrini, M. Shimizu, D. Comoretto, A. Pucci, *Mater. Chem. Front.* **2019**, *3*, 429.
[227] P. P. C. Verbunt, A. Kaiser, K. Hermans, C. W. M. Bastiaansen, D. J. Broer, M. G. Debije, *Adv. Funct. Mater.* **2009**, *19*, 2714.
[228] R. W. MacQueen, Y. Yap Cheng, R. G. C. R. Clady, T. W. Schmid, *Opt. Express* **2010**, *18*, A161.
[229] S. McDowall, B. L. Johnson, D. L. Patrick, *J. Appl. Phys.* **2010**, *108*, 053508.
[230] C. L. Mulder, P. D. Reusswig, A. M. Velázquez, H. Kim, C. Rotschild, M. A. Baldo, *Opt. Express* **2010**, *18*, A70.
[231] M. G. Debije, C. Menelaou, L. M. Herz, A. P. H. J. Schenning, *Adv. Opt. Mater.* **2014**, *2*, 687.
[232] P. P. C. Verbunt, T. M. de Jong, D. K. G. de Boer, D. J. Broer, M. G. Debije, *Eur. Phys. J. Appl. Phys.* **2014**, *67*, 10201.
[233] B. Zhang, C. Gao, H. Soleimaninejad, J. M. White, A. S. Trevor, D. J. Jones, K. P. Ghiggino, W. W. H. Wong, *Chem. Mater.* **2019**, *31*, 3001.
[234] L. R. Dalton, P. A. Sullivan, D. H. Bale, *Chem. Rev.* **2010**, *110*, 25.
[235] W. Stahl, V. Wittwer, A. Goetzberger, *Sol. Energy* **1986**, *36*, 27.
[236] S. Melnik, A. H. Rawicz, *Appl. Opt.* **1997**, *36*, 9025.
[237] M. H. Sanders, R. J. Sedwick, *J. Spacecr. Rockets* **2019**, *56*, 1831.
[238] Y. Yang, I. D. W. Samuel, G. A. Turnbull, *Adv. Mater.* **2009**, *21*, 3205.
[239] N. S. Makarov, K. Ramasamy, A. Jackson, A. Velarde, C. Castaneda, N. Archuleta, D. Hebert, M. R. Bergren, H. McDaniel, *ACS Nano* **2019**, *13*, 9112.
[240] P. D. Swift, G. B. Smith, J. B. Franklin, presented at SPIE Conf. on Solar Optical Materials XVI, Denver, CO July **1999**.
[241] A. A. Earp, G. B. Smith, J. Franklin, P. Swift, *Sol. Energy Mater. Sol. Cells* **2004**, *84*, 411.
[242] C. Lamnatou, D. Chemisana, *Renewable Sustainable Energy Rev.* **2013**, *27*, 175.
[243] A. Novoplansky, T. Sachs, D. Cohen, R. Bar, J. Bodenheimer, R. Reisfeld, *Sol. Energy Mater. Sol. Cells* **1990**, *21*, 17.
[244] S. M. El-Bashir, F. F. Al-Harbi, H. Elburaih, F. Al-Faifi, I. S. Yahia, *Renewable Energy* **2016**, *85*, 928.
[245] M. Hammam, M. K. El-Mansy, S. M. El-Bashir, M. G. El-Shaarawy, *Desalination* **2007**, *209*, 244.
[246] M. Raeisossadati, N. R. Moheimani, D. Parlevliet, *Algal Res.* **2020**, *45*, 101771.
[247] M. Raeisossadati, N. R. Moheimani, D. Parlevliet, *Bioresour. Technol.* **2019**, *291*, 121801.
[248] T. J. J. Meyer, T. Markvart, *J. Appl. Phys.* **2009**, *105*, 063110.
[249] D. Cambié, F. Zhao, V. Hessel, M. G. Debije, T. No, *Angew. Chem., Int. Ed.* **2017**, *56*, 1050.
[250] D. Cambié, J. Dobbelaar, P. Riente Paiva, J. Vanderspikken, C. Shen, P. H. Seeberger, K. Gilmore, M. G. Debije, T. Noël, *Angew. Chem., Int. Ed.* **2019**, *58*, 14374.
[251] D. Cambié, F. Zhao, V. Hessel, M. G. Debije, T. Noël, *React. Chem. Eng.* **2017**, *2*, 561.
[252] F. Zhao, D. Cambié, J. Janse, E. Wieland, K. P. L. Kuijpers, V. Hessel, M. G. Debije, T. Noël, *ACS Sustainable Chem. Eng.* **2018**, *6*, 422.
[253] G. X. de Oliveira, J. O. B. Lira, D. Cambié, T. Noël, H. G. Riella, N. Padoina, C. Soares, *Chem. Eng. Res. Des.* **2020**, *153*, 626.
[254] G. Liu, B. Sun, H. Li, Y. Wang, H. Zhao, *J. Mater. Chem. A.* **2019**, *7*, 18529.
[255] B. Norton, P. C. Eames, T. K. Mallick, M. J. Huang, S. J. McCormack, J. D. Mondol, Y. G. Yohanis, *Sol. Energy* **2011**, *85*, 1629.
[256] I. Cerón, E. Caamaño-Martín, F. J. Neila, *Renewable Energy* **2013**, *58*, 127.
[257] N. Aste, L. C. Tiagliabue, P. Palladino, D. Testa, *Sol. Energy* **2015**, *114*, 174.
[258] E. Biyik, M. Araz, A. Hepbasli, M. Shahrestani, R. Yao, L. Shao, E. Essah, A. C. Oliveira, T. del Caño, E. Rico, J. L. Lechón, L. Andrade, A. Mendes, Y. B. Atlı, *Eng. Sci. Technol, Int. J.* **2017**, *20*, 833.
[259] N. Aste, M. Buzzetti, C. Del Pero, R. Fusco, F. Leonforte, D. Testa, *J. Cleaner Prod.* **2019**, *219*, 35.
[260] M. Kanellis, M. M. de Jong, L. Slooff, M. G. Debije, *Renewable Energy* **2017**, *103*, 647.
[261] M. G. Debije, C. Tzikas, V. A. Rajkumar, M. M. de Jong, *Renewable Energy* **2017**, *113*, 1288.
[262] A. H. M. E. Reinders, G. D. de la Gree, A. Papadopoulos, A. Rosemann, M. G. Debije, M. Cox, Z. Krumer, in *2016 IEEE 43rd Photovoltaic Specialists Conf. (PVSC)*, IEEE, Piscataway, NJ **2016**, p. 3447.
[263] A. Reinders, M. G. Debije, A. Rosemann, *IEEE J. Photovoltaics* **2017**, *7*, 1663.
[264] F. M. Vossen, M. P. J. Aartsa, M. G. Debije, *Energy Build.* **2016**, *113*, 123.
[265] M. G. Debije, V. A. Rajmunkar, *Sol. Energy* **2015**, *122*, 334.
[266] A. Kerrouche, D. A. Hardy, D. Ross, B. S. Richards, *Sol. Energy Mater. Sol. Cells* **2014**, *122*, 99.
[267] A. Renny, C. Yang, R. Anthony, R. R. Lunt, *J. Chem. Educ.* **2018**, *95*, 1161.
[268] A. Reinders, R. Kishore, L. Slooff, W. Eggink, *Jpn J. Appl. Phys.* **2018**, *57*, 08RD10.
[269] J. ter Schiphorst, M. L. M. K. H. Y. K. Cheng, M. van der Heijden, R. L. Hageman, E. L. Bugg, T. J. L. Wagenaar, M. G. Debije, *Energy Build.* **2020**, *207*, 109625.
[270] C. Yang, R. R. Lunt, *Adv. Opt. Mater.* **2017**, *5*, 1600851.
[271] C. J. Traverse, R. Pandey, M. C. Barr, R. R. Lunt, *Nat. Energy* **2017**, *2*, 849.
[272] Y. Zhou, D. Benetti, Z. Fan, H. Zhao, D. Ma, A. O. Govorov, A. Vomiero, F. Rosei, *Adv. Energy. Mater.* **2016**, *6*, 1501913.
[273] J. W. E. Wiegman, E. van der Kolk, *Sol. Energy Mater. Sol. Cells* **2012**, *103*, 41.
[274] C. Yang, M. Moemeni, M. Bates, W. Sheng, B. Borhan, R. R. Lunt, *Adv. Opt. Mater.* **2020**, *8*, 1901536.

[275] J. ter Schiphorst, A. M. Kendhale, M. G. Debije, C. Menelaou, L. M. Herz, A. P. H. J. Schenning, *Chem. Mater.* **2014**, *26*, 3876.
[276] J. A. H. P. Sol, G. H. Timmermans, A. J. van Breugel, A. P. H. J. Schenning, M. G. Debije, *Adv. Energy Mater.* **2018**, *8*, 1702922.
[277] G. H. Timmermans, B. W. H. Saes, M. G. Debije, *Appl. Opt.* **2019**, *58*, 9823.
[278] C. Wang, S. Hirst, R. Winston, in *Nonimaging Optics: Efficient Design for Illumination and Solar Concentration VIII* (Eds: R. Winston, J. M. Gordon), SPIE, Bellingham, WA **2018**, p. 81240O.
[279] N. Aste, L. C. Tagliabue, C. Del Pero, D. Testa, R. Fusco, *Renewable Energy* **2015**, *76*, 330.
[280] V. Wittwer, K. Heidler, A. Zastrow, A. Goetzberger, *J. Lumin.* **1981**, *24–25*, 873.
[281] L. Desmet, A. J. M. Ras, D. K. G. de Boer, M. G. Debije, *Opt. Lett.* **2012**, *37*, 3087.

Jean Roncali received his Ph.D. on luminescent solar concentrators in 1984 in Paris under the supervision of Francis Garnier. After successive positions as engineer and researcher in the Laboratory of Molecular Materials of CNRS, in 1991, he moved to the University of Angers and created the group Linear Conjugated Systems as research director. Presently, as associated senior scientist at the Babes-Bolyai University of Cluj-Napoca (Romania) and CNRS emeritus research director, his research deals with functional π-conjugated systems for electrode materials, photonics, molecular electronics, and energy conversion and storage.